PHYSICAL REVIEW D **81,** 016001 (2010)

Light-meson spectroscopy and combined analysis of processes with pseudoscalar mesons

Yu. S. Surovtsev*
Bogoliubov Laboratory of Theoretical Physics, JINR, Dubna 141980, Russia

P. Bydžovský†
Nuclear Physics Institute, ASCR, Řež near Prague 25068, Czech Republic

R. Kamiński‡
Institute of Nuclear Physics, PAS, Cracow 31342, Poland

M. Nagy§
Institute of Physics, Slovak Academy of Sciences, Dubravska cesta 9, 845 11 Bratislava, Slovak Republic
(Received 12 August 2009; published 6 January 2010)

The status and parameters of the scalar, vector, and tensor mesonic resonances are obtained in the multichannel analysis of processes $\pi\pi \to \pi\pi$, $K\bar{K}$, $\eta\eta$, and $\eta\eta'$ and compared with other results. For example, we obtained the $f_0(600)$ meson with mass 774 ± 15 MeV and width 988 ± 36 MeV (the pole position on sheet II is $596 - i494$ MeV) and the first ρ-like meson with mass 1275 ± 32 MeV and total width 304 ± 24 MeV, which differ significantly from the mean value 1459 ± 11 MeV cited in the Particle Data Group tables. Spectroscopic implications from results of these analyses and possible classification of the resonance states in terms of the SU(3) multiplets are also discussed.

DOI: 10.1103/PhysRevD.81.016001 PACS numbers: 11.55.Bq, 13.75.Lb, 14.40.−n

I. INTRODUCTION

The spectroscopy of light mesons is very important for understanding the strong interactions at low energies. Here scalar mesons have a special status because they possess the vacuum quantum numbers and, therefore, they can mediate the vacuum influence on the hadronic spectrum by means of possible ''direct'' transitions. In turn, the lightest scalar mesons act on the vacuum through a possible condensation into it. Therefore, the scalars are a very exciting and much discussed topic in the light hadron physics. However, present knowledge about the nature of discovered states in the scalar mesonic sector is still rather incomplete[1] and their parameters are known with rather large spread [1]. This especially concerns the $f_0(600)/\sigma$ meson whose existence was doubted for a long time and which now can be considered to be discovered. For example, the $f_0(600)$ mass, obtained in the Breit-Wigner or K-matrix approaches, ranges in various analyses from about 400 to 1200 MeV [1]. The $f_0(600)$ width also ranges from a very small value, 35 ± 12 MeV [2], to a very large one, 800–1000 MeV [3–10]. It is clear that due to the large spread of parameters, it is difficult to determine the nature of the $f_0(600)$. Note that for the mass of the σ meson, there is a prediction by Weinberg [11] on the basis of mended symmetry that this state should be almost degenerate with the ρ-meson mass. Saturating the superconvergence sum rules, one finds that the σ-meson width is 4.5 times larger than the ρ-meson width [12]. On the other hand, in studies of QCD sum rules [13] one found a scalar-isoscalar meson with a mass about 1000 MeV which is the state of the gluonium nature with the $\pi\pi$-decay width about 500 MeV. This is in agreement with the recent unquenched-lattice simulation using dynamical fermions [14]. However, there are recent calculations on the quenched anisotropic lattices of the glueball spectrum where the mass of the lowest glueball is about 1710 MeV [15]. It seems that a question about the lowest glueball mass has not yet been solved in the lattice simulations.

As to the width of the glueball, e.g., in the Ellis-Lánik approach [16] of an effective QCD Lagrangian with broken scale and chiral symmetry, where a glueball is introduced to theory as a dilaton and its existence is related to the breaking of the scale symmetry in QCD, the $\pi\pi$-decay width is estimated using classical low energy theorems yielding $\Gamma(G/\text{glueball} \to \pi\pi) \approx 0.6\ \text{GeV} \times (m_G/1\ \text{GeV})^5$, where m_G is the glueball mass. Therefore, it is important for estimating the width if m_G is smaller or bigger than 1 GeV. Though the use of the Ellis-Lanik formula is doubtful above 1 GeV, a tendency for the glueball to be wide is apparently seen. This is supported by arguments from Anisovich [17] that the glueball width is larger than the ones of surrounding $q\bar{q}$ states. On the other hand, the authors of Ref. [18] analyzed the two-

*surovcev@theor.jinr.ru
†bydz@ujf.cas.cz
‡Robert.Kaminski@ifj.edu.pl
§fyzinami@unix.savba.sk
[1]Here we confine ourselves to consideration of states below 1900 MeV.

pseudoscalar and two-photon decays of the scalars between 1–2 GeV in the framework of a chiral Lagrangian, where the glueball has been included as a flavor-blind composite mesonic field, and found the glueball to be rather narrow in accordance with the earlier issues of Ref. [19]. It seems that the question about the glueball width is not yet answered.

The study of a remarkable resonance phenomenon in the scalar-isoscalar mesonic sector, the $f_0(980)$, still brings surprises. This state has been earlier assigned to the conventional $q\bar{q}$ [20–23] or $q^2\bar{q}^2$ nonets [24,25] and also interpreted as a $K\bar{K}$ molecule [26–28] or even as a glueball [29]. Now additional arguments have appeared [30] in favor of the 4-quark nature of $f_0(980)$ and $a_0(980)$ mesons based on interpretation of the experimental data on the decays $\phi \to \gamma\pi^0\pi^0$, $\gamma\pi^0\eta$ [31]. In our previous model-independent combined analysis of experimental data on processes $\pi\pi \to \pi\pi$, $K\bar{K}$, and $\eta\eta$, based on analyticity and unitarity, we have concluded that the $f_0(980)$ might be a bound $\eta\eta$ state [10,32].

As to the $f_0(1370)$ meson, e.g., the authors of works [33] did not find compelling evidence for the existence of the $f_0(1370)$ as a single resonance in their phenomenological analysis of the spectrum of light scalar mesons. In our earlier work [7] we also clashed with the fact that the best combined description of the isoscalar S-wave channel of the processes $\pi\pi \to \pi\pi$, $K\bar{K}$ is obtained without this resonance, and we have shown that the $K\bar{K}$ scattering length is very sensitive to whether the $f_0(1370)$ exists or not. On the other hand, Bugg [34] indicated a number of data apparently requiring the existence of the $f_0(1370)$. These are, in the first place, the Crystal Barrel data on $\bar{p}p \to \eta\eta\pi^0$ [35] and on $\bar{p}p \to 3\pi^0$ [36] and also the BES data on $J/\psi \to \phi\pi^+\pi^-$ [37]; the $f_0(1370)$ appears also in the GAMS data for $\pi^+\pi^- \to \pi^0\pi^0$ at large $|t|$ [38]. For example, in [39] it is shown within the so-called ''hidden gauge formalism'' that the $f_0(1370)$ might be dynamically generated from the $\rho\rho$ interaction or, in simpler words, the $\rho\rho$ molecular state.

An interesting situation has turned up as to the scalar state in the 1500-MeV region. In all our previous model-independent analyses of data on processes $\pi\pi \to \pi\pi$, $K\bar{K}$, $\eta\eta$, and $\eta\eta'$ with using different uniformizing variables [6–10,32,40], we saw the wide state $f_0(1500)$, whereas in many works of other authors, analyzing mainly meson production and decay processes and cited in the Particle Data Group (PDG) issue on the $f_0(1500)$ listing [1], the rather narrow $f_0(1500)$ is obtained. Therefore, in some accordance with the results of the combined K-matrix analysis [41] of the GAMS data on $\pi^- p \to \pi^0\pi^0 n$, $\eta\eta n$, and $\eta\eta' n$ [42–44], BNL data on $\pi^- p \to K\bar{K}n$ [45], and Crystal Barrel data on $p\bar{p}(\text{at rest}) \to \pi^0\pi^0\pi^0$, $\pi^0\pi^0\eta$, $\pi^0\eta\eta$ [46–48], which say that in the 1500-MeV region there are the narrow $f_0(1500)$ and very wide $f_0(1530^{+90}_{-250})$, we have suggested [8] that the wide $f_0(1500)$, observed in the multichannel $\pi\pi$ scattering, indeed, is a superposition of two states, wide and narrow. The latter is observed just in the processes of decay and production of mesons. We suppose [7] that the $f_0(1500)$ is practically the eighth component of the $q\bar{q}$ octet mixed with the glueball being dominant in this state. This is in accordance with the Anisovich arguments on the glueball width [17] and with the fact that the $f_0(1500)$ is coupled with the approximately equal strength with the $\pi\pi$, $K\bar{K}$, and $\eta\eta$ systems [6–10,32].

As to the $f_0(1710)$, it has most likely the dominant $s\bar{s}$ component (see, e.g., Refs. [1,7,49]). Note, however, that QCD sum rules [50] and the K-matrix method [51] showed both the $f_0(1500)$ and $f_0(1710)$ to be mixed states with a large admixture of the glueball component.

Predictions, obtained in the scalar sector, are practically not disguised by the kinematic factors. This is especially important because the f_0 mesons are the most direct carriers of information about the QCD vacuum. It seems that our inadequate understanding of the QCD vacuum and of its influence on the hadron spectrum and properties of hadrons is the main reason why a completely satisfactory assignment of the scalar mesons to SU(3) nonets is not proposed up to now, although there is a number of interesting conjectures, e.g., in Refs. [52–56].

The investigation of vector mesons is also an up-to-date subject due to their role in forming the electromagnetic structure of particles and because our knowledge about these mesons is still too incomplete [e.g., in the PDG tables [1] the mass of $\rho(1450)$ is ranging from 1250 to 1582 MeV]. The question of existence of the state $\rho(1250)$ is raised again to an agenda by a number of investigations [32,57,58]. The $\rho(1250)$ meson (as the first radial excitation of the $I^G J^{PC} = 1^+1^{--}$ $q\bar{q}$ state) was discussed actively some time ago [59,60]. Later the evidence for its existence was obtained by the LASS Collaboration [61] and in work [62] when analyzing the processes $e^+e^- \to \pi^+\pi^-$, $\rho 2\pi$, $\omega\pi$, and $\eta 2\pi$, and the $\pi\pi$ scattering. Recently an additional confirmation for this state was given in the reanalyses of data on the $\pi\pi$ scattering [32,57] and reaction $e^+e^- \to \omega\pi^0$ [58]. If the $\rho(1250)$ is interpreted as the first radial excitation of the ρ meson, then it lies well on the corresponding linear trajectory with a universal slope on the (n, m^2) plane (n is the radial quantum number of the $q\bar{q}$ state) [51], whereas the $\rho(1450)$ turns out to be considerably higher than this trajectory. The $\rho(1250)$ and the isodoublet $K^*(1410)$ are well located to the octet of first radial excitations. The mass of the latter should be by about 150 MeV larger than the mass of the former. Then the Gell-Mann–Okubo (GMO) formula

$$3m^2_{\omega'_8} = 4m^2_{K^{*\prime}} - m^2_{\rho'}$$

gives the value $m_{\omega'_8} = 1460$ MeV that is fairly compatible with the mass of the first ω-like meson $\omega(1420)$, for which

one obtains the values in the range 1350–1460 MeV, cited in the PDG tables [1].

In our previous work [32,57] it was shown that the existence of the $\rho(1450)$ [together with $\rho(1250)$] does not contradict the $\pi\pi$-scattering data. This issue was obtained using both our model-independent method [40] in the 2-channel consideration of the $\pi\pi$ scattering and the Breit-Wigner forms in the 5-channel consideration. In the $q\bar{q}$ picture, the $\rho(1450)$ might be the first $^3D_1$ state with, possibly, the isodoublet $K^*(1680)$ in the corresponding octet. From the GMO formula, we should obtain the value 1750 MeV for the mass of the eighth component of this octet. This corresponds to one of the observations of the second ω-like meson which is cited in the PDG tables under the $\omega(1650)$ and has the mass, obtained in various works, from 1606 to 1840 MeV.

The suggested picture for the first two ρ-like mesons is consistent with predictions of the quark model [63]. In [60] the discussed mass spectrum for radially excited ρ and K^* mesons was obtained using a rather simple mass operator under the natural assumption that the parameters of spin-spin splitting in radial excitations as compared to the splitting in the ground states change by a factor proportional to the ratio of the corresponding wave functions ''at zero.'' Of course, if the existence of the $\rho(1250)$ is confirmed, some quark potential models, e.g. in Ref. [52], will require substantial revisions, because the first ρ-like meson is usually predicted about 200 MeV higher than this state. In addition, the first K^*-like meson is obtained in the indicated quark model at 1580 MeV, whereas the corresponding well-established resonance has a mass of only 1410 MeV [1]. To the point, in the isoscalar-scalar and isoscalar-tensor sectors, there are also disagreements with predictions of the indicated model, e.g., with respect to the $f_0(600)$ and $f_0(1500)$ in the scalar sector and to the second $q\bar{q}$ nonet in the tensor sector [10,32].

In the tensor sector, among the 13 resonances discussed in the literature, the nine states [$f_2(1430)$, $f_2(1565)$, $f_2(1640)$, $f_2(1810)$, $f_2(1910)$, $f_2(2000)$, $f_2(2020)$, $f_2(2150)$, and $f_2(2220)$] must be confirmed in various experiments and analyses [1]. For example, in the analysis [64] of $p\bar{p} \to \pi\pi$, $\eta\eta$, $\eta\eta'$, five resonances—$f_2(1920)$, $f_2(2000)$, $f_2(2020)$, $f_2(2240)$, and $f_2(2300)$—have been obtained, one of which, $f_2(2000)$, is a candidate for the glueball. In [10,32], where the data on processes $\pi\pi \to \pi\pi$, $K\bar{K}$, $\eta\eta$, $\eta\eta'$ in the channels with the quantum numbers $I^GJ^{PC} = 0^+2^{++}$ were analyzed using the 4-channel Breit-Wigner forms, we have confirmed the existence of the states $f_2(1450)$, $f_2(1565)$, $f_2(1810)$, $f_2(2000)$, and $f_2(2220)$ and have seen the $f_2(1730)$, related to the statistically valued experimental points. We have also shown that the allowance for the $f_2(2020)$ in the analysis permits us to interpret $f_2(2000)$ as the glueball, because in this case all the obtained ratios of the partial widths of this state are in the limits corresponding to the tensor glueball, which are derived in Ref. [64] on the basis of the $1/N_c$-expansion rules.

In view of the above discussion, it is clear that resonance parameters should be obtained, if possible, in a model- and dynamic-assumption-independent way. Here, we present results of the coupled-channel analysis of data on processes $\pi\pi \to \pi\pi$, $K\bar{K}$, $\eta\eta$, $\eta\eta'$ in the channels with $I^GJ^{PC} = 0^+0^{++}$ and 0^+2^{++} and on the $\pi\pi$ scattering in the channel with $I^GJ^{PC} = 1^+1^{--}$. In the 3-channel considerations of the scalar and vector sectors, we have used our model-independent method [40], based on the first principles (analyticity and unitarity) directly applied to the analysis of experimental data. In the 4-channel consideration of the tensor sector, we enforced the multichannel Breit-Wigner forms to generate the resonance poles and zeros in the S matrix. Note that the former approach is more preferable because it is very sensitive to data and permits us to avoid introducing theoretical prejudice to extracted parameters of resonances. Furthermore, in the latter approach it is impossible to describe adequately some types of the multichannel resonances [40]. However, the model-independent method is limited to the possibility of using only two and three coupled channels; therefore, in more general cases, one has to use other approaches. Considering the obtained arrangement of resonance poles on the Riemann surface, obtained coupling constants with channels, and resonance masses we draw particular conclusions about the nature of the investigated states.

The layout of this paper is as follows. In Sec. II, we outline the three-coupled-channel formalism, determine the pole clusters on the Riemann surface as characteristics of multichannel states, introduce a corresponding uniformizing variable, and consider a representation of the multichannel resonances of various types on the uniformization plane. In Sec. III, we analyze the experimental data [65–67] on the isovector P wave of $\pi\pi$ scattering using the 3-channel model-independent method [40]. In Sec. IV, we present results of the improved combined 3-channel model-independent analysis of data [67–69,43,44] on processes $\pi\pi \to \pi\pi$, $K\bar{K}$, $\eta\eta$, and $\eta\eta'$ in the isoscalar-scalar sector. In Sec. V, we analyze simultaneously (or jointly) the data [67,70] on processes $\pi\pi \to \pi\pi$, $K\bar{K}$, and $\eta\eta$ in the isoscalar-tensor sector, using the multichannel Breit-Wigner forms. In Sec. VI, we summarize our conclusions on the basis of realized analyses and discuss the obtained results and their spectroscopic implications.

II. METHOD OF ANALYSIS

We used both the model-independent method of analysis [40] (in the scalar and vector sectors) and the Breit-Wigner one (in the tensor sector). In both methods, we parametrized the S-matrix elements S_{ab}, where $a, b = 1, 2, \ldots, N$ denote channels, using the Le Couteur–Newton relations [71]. These relations express the S-matrix elements of all coupled processes in terms of the Jost matrix determinant

$d(k_1, \ldots, k_N)$ that is a real analytic function with the only square-root branch points at the channel momenta $k_a = 0$[2]:

$$S_{aa} = \frac{d(k_1, \ldots, k_{a-1}, -k_a, k_{a+1}, \ldots, k_N)}{d(k_1, \ldots, k_N)}, \qquad S_{aa}S_{bb} - S_{ab}^2 = \frac{d(k_1, \ldots, k_{a-1}, -k_a, k_{a+1}, \ldots, k_{b-1}, -k_b, k_{b+1}, \ldots, k_N)}{d(k_1, \ldots, k_N)}. \tag{1}$$

(We wrote down those relations which we used in practice.) The real analyticity implies

$$d(s^*) = d^*(s) \quad \text{for all } s, \tag{2}$$

and the N-channel unitarity requires the following relations to hold for physical s values:

$$N \text{ relations } |d(k_1, \ldots, -k_a, \ldots, k_N)| \le |d(k_1, \ldots, k_N)|, \tag{3}$$

and

$$|d(-k_1, \ldots, -k_a, \ldots, -k_N)| = |d(k_1, \ldots, k_a, \ldots, k_N)|. \tag{4}$$

The N-channel S-matrix is determined on the 2^N-sheeted Riemann surface. Further we discuss the 3-channel S-matrix determined on the 8-sheeted Riemann surface. The matrix elements S_{ab} have the right-hand cuts along the real axis of the s complex plane (s is the invariant total energy squared), starting at the coupled-channel thresholds s_a ($a = 1, 2, 3$), and the left-hand cuts related to the crossed channels. The Riemann-surface sheets are numbered according to the signs of analytic continuations of the quantities $\sqrt{s - s_a}$ as follows:

$$\begin{aligned}&\text{signs}(\text{Im}\sqrt{s - s_1}, \text{Im}\sqrt{s - s_2}, \text{Im}\sqrt{s - s_3})\\ &= +++, -++, --+, +-+, +--, ---,\\ &\quad -+-, ++-\end{aligned}$$

correspond to sheets I, II,..., VIII, respectively.

In the model-independent approach, the resonance representations on the Riemann surfaces are obtained with the help of formulas from Refs. [9,40], expressing analytic continuations of the S-matrix elements to unphysical sheets in terms of those on sheet I that have only the zeros of resonances (beyond the real axis), at least, around the physical region. Then, starting from the resonance zeros on sheet I, one can obtain an arrangement of poles and zeros, representing the resonance, on the whole Riemann surface.

In the 3-channel case, we obtain seven types of resonances corresponding to seven possible situations when there are resonance zeros on sheet I only in S_{11} (a); S_{22} (b); S_{33} (c); S_{11} and S_{22} (d); S_{22} and S_{33} (e); S_{11} and S_{33} (f); and S_{11}, S_{22}, and S_{33} (g).

[2]Other authors have also used the parametrizations with the Jost functions in analyzing the S-wave $\pi\pi$ scattering in the one-channel [72] and two-channel [73] approaches.

A resonance of every type is represented by a pair of complex-conjugate clusters (of poles and zeros on the Riemann surface). A necessary and sufficient condition for existence of the multichannel resonance is its representation by one of the types of pole clusters. Note that whereas cases (a)–(c) can be simply related to the representation of resonances by the Breit-Wigner forms, cases (d)–(g) are practically lost in the Breit-Wigner description. The cluster type is related to the nature of state. For example, if we consider the $\pi\pi$, $K\bar{K}$, and $\eta\eta$ channels, then a resonance which is coupled relatively more strongly to the $\pi\pi$ channel than to the $K\bar{K}$ and $\eta\eta$ ones is described by the cluster of type (a). If the resonance is coupled more strongly to the $K\bar{K}$ and $\eta\eta$ channels than to the $\pi\pi$ one, then it is represented by the cluster of type (e) (say, the state with the dominant $s\bar{s}$ component). The glueball must be represented by the cluster of type (g) as a necessary condition for the ideal case, if this state lies above the thresholds of considered channels.

We can distinguish, in a model-independent way, a bound state of colorless particles (e.g., $K\bar{K}$ molecule) and a $q\bar{q}$ bound state. In the 1-channel case, the existence of the particle bound state means the presence of the pole on the real axis under the threshold on the physical sheet. In the 3-channel case, the bound state in channel 3 ($\eta\eta$) that, however, can decay into channels 1 ($\pi\pi$ decay) and 2 ($K\bar{K}$ decay), is represented by the pair of complex-conjugate poles on sheet II and by shifted poles on sheet III under the $\eta\eta$ threshold without the corresponding poles on sheets VI and VII. According to this test [40,73], earlier in Ref. [40], the interpretation of the $f_0(980)$ state as the $K\bar{K}$ molecule has been rejected because this state is represented by the cluster of type (a) in the 2-channel analysis of processes $\pi\pi \to \pi\pi$ and $K\bar{K}$ and, therefore, it does not satisfy the necessary condition to be the $K\bar{K}$ molecule.

Unlike the standard dispersion relation approach, in our model-independent method, we use an advantage of the fact that the amplitude is a one-valued function on the Riemann surface. To this end, a uniformizing variable is applied, which maps the Riemann surface onto a plane. In the 2-channel case, this can be made using the inverse Zhukovskij transformation [40], in which the thresholds of two channels are taken into account, or using the variable, in which the left-hand branch point related to the crossed channels, e.g. at $s = 0$ [7,57], is included in addition to the two indicated right-hand threshold branch points. As was indicated repeatedly (see, e.g., Ref. [74]), many analyses could be exposed to a well-grounded criti-

cism (especially with the point of view of proof of the resonance existence) because the wide-resonance parameters are strongly controlled by the nonresonant background; particularly this is related to low-lying states. In particular, the allowance for the left-hand branch point, related to the crossed channels, serves for a solution to this problem. For example, in our previous combined analysis [7] of the processes $\pi\pi \to \pi\pi$ and $K\bar{K}$ in the isoscalar-scalar sector by method of the uniformizing variable which includes two threshold branch points and the left-hand one at $s = 0$, we obtained a parameterless description of the $\pi\pi$ background due to the account of the indicated left-hand branch point. Moreover, we have shown that the large background, obtained in earlier analyses of the S-wave $\pi\pi$ scattering [40], hides, in reality, the σ meson below 1 GeV.

The allowance for the third threshold branch point in the uniformizing variable in the 3-channel consideration should also diminish the background dependence of obtained results. However, with the help of a simple mapping, a function, determined on the 8-sheeted Riemann surface, can be uniformized only on torus. This is unsatisfactory for our purpose. Therefore, we neglect the influence of the lowest $(\pi\pi)$ threshold branch point (however, unitarity on the $\pi\pi$ cut is taken into account). An approximation like this means the consideration of the nearest to the physical region semisheets of the Riemann surface of the S matrix. In fact, we construct a 4-sheeted model of the initial 8-sheeted Riemann surface approximating it in accordance with our approach of a consistent account of the nearest singularities on all the relevant sheets. In practice the disregard of influence of the $\pi\pi$-threshold branch point denotes that we do not describe some region near the threshold. This is justified because for the analysis of this region, the 2-channel and even 1-channel considerations are sufficient. So, our corresponding uniformizing variable has the form:

$$w = \frac{\sqrt{s - s_2} + \sqrt{s - s_3}}{\sqrt{s_3 - s_2}}. \tag{5}$$

It maps our model of the 8-sheeted Riemann surface onto the w plane divided into two parts by a unit circle centered at the origin (Figs. 1). Sheets I (III), II (IV), V (VII), and VI (VIII) are mapped onto the exterior (interior) of the unit disk in the 1st, 2nd, 3rd, and 4th quadrants, respectively. The physical region extends from the point $w_{\pi\pi}$ on the imaginary axis (the first $\pi\pi$ threshold, corresponding s_1, $|w_{\pi\pi}| > 1$) down this axis to the point i on the unit circle (the second threshold), farther along the unit circle clockwise in the 1st quadrant to point 1 on the real axis (the third threshold) and then along the real axis to ∞. The representation of resonances of types (a)–(e), and (g) by the pole clusters in S_{11} is shown in Figs. 1(a)–1(f), respectively. (These types of resonances are used in the following when describing four indicated processes.) In this case the resonance poles ($*$) and zeros ($\circ$) are symmetric to each other with respect to the imaginary axis. The "pole-zero" symmetry is required for elastic unitarity on the $(\pi\pi, i)$ interval.

Note that, due to the use of the uniformizing variable method, we can realize the one more important element of our approach, namely, representation of multichannel resonances (depending on their nature) by one of the types of the above pole clusters.

The Le Couteur–Newton relations are modified by taking into account the used model of the Riemann surface (note that on the w plane the points w_0, $-w_0^{-1}$, $-w_0$, and w_0^{-1} correspond to the s-variable point s_0 on sheets I, IV, V, and VIII, respectively) [40]:

$$\begin{aligned} S_{11} &= \frac{d^*(-w^*)}{d(w)}, \qquad S_{22} = \frac{d(-w^{-1})}{d(w)}, \\ S_{33} &= \frac{d(w^{-1})}{d(w)}, \qquad S_{11}S_{22} - S_{12}^2 = \frac{d^*(w^{*-1})}{d(w)}, \\ S_{11}S_{33} - S_{13}^2 &= \frac{d^*(-w^{*-1})}{d(w)}, \qquad S_{22}S_{33} - S_{23}^2 = \frac{d(-w)}{d(w)}. \end{aligned} \tag{6}$$

Since, in the model of the Riemann surface, only the semisheets of the initial Riemann surface nearest to the physical region are considered, one can say nothing regarding the property of the real analyticity of the amplitudes. The 3-channel unitarity requires the following relations to hold for physical w values:

$$\begin{aligned} &|d(-w^*)| \le |d(w)|, \qquad |d(-w^{-1})| \le |d(w)|, \\ &|d(w^{-1})| \le |d(w)|, \qquad |d(w^{*-1})| \le |d(w)|, \\ &|d(-w^{*-1})| \le |d(w)|, \qquad |d(-w)| \le |d(w)|. \end{aligned} \tag{7}$$

Though one can put a task of uniformization of the whole S matrix as it was made in our previous 2-channel consideration [7] of processes $\pi\pi \to \pi\pi$ and $K\bar{K}$, here it is convenient to represent the S matrix as

$$S = S_B S_{\text{res}}, \tag{8}$$

where S_B describes the background, S_{res} the resonance contributions, and to apply the uniformization procedure and formulas (6) for S_{res}; for S_B, Eqs. (1) are used. The d function for the resonance part is

$$d_{\text{res}}(w) = w^{-(M/2)} \prod (w + w_r^*), \tag{9}$$

where the product includes all zeros w_r of the chosen resonances, and M is the number of resonance zeros.

As the data below show, we use the results of phase analyses which are given for phase shifts of the amplitudes δ_{ab} and for moduli of the S-matrix elements $\eta_{ab} = |S_{ab}|$ $(a, b = 1, 2, 3)$:

$$S_{aa} = \eta_{aa} e^{2i\delta_{aa}}, \qquad S_{ab} = \eta_{ab} e^{i\phi_{ab}}. \tag{10}$$

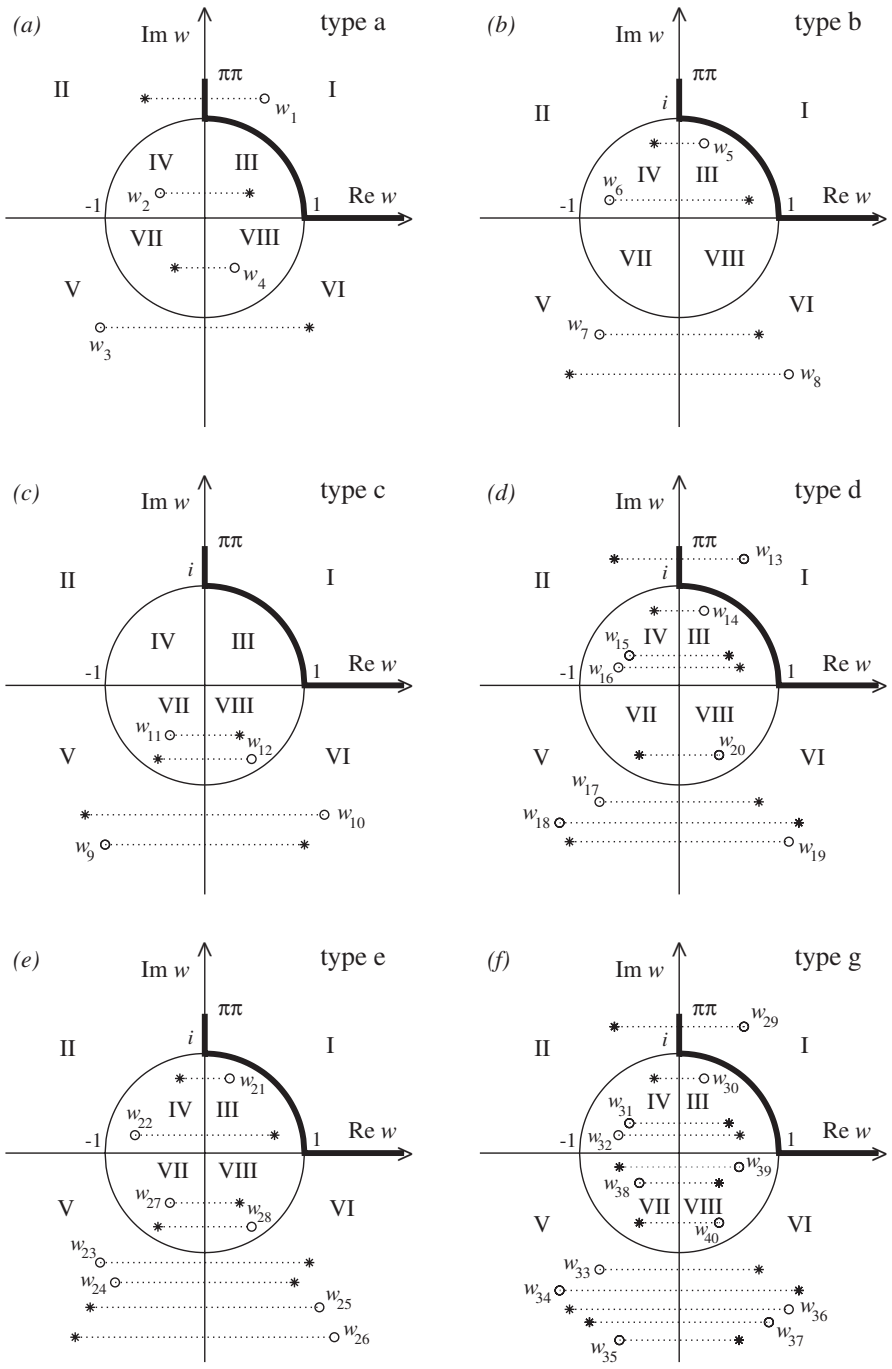

FIG. 1. Uniformization w plane for the 3-channel $\pi\pi$ scattering S-matrix element: the Roman numerals I–VIII mark images of the corresponding sheets of the Riemann surface; the thick lines denote the physical region where the points $\pi\pi$, i, and 1 correspond to the $\pi\pi$, 2nd, and 3rd thresholds, respectively. Representation of resonances of types (a)–(e), and (g) by poles ($*$) and zeros ($\circ$) is shown in (a)–(f), respectively. The resonance zeros are labeled by w_i.

If below the third threshold there is the 2-channel unitarity, then the relations

$$\eta_{11} = \eta_{22}, \qquad \eta_{12} = (1 - \eta_{11}^2)^{1/2}, \qquad \phi_{12} = \delta_{11} + \delta_{22} \tag{11}$$

are fulfilled in this energy region.

III. ANALYSIS OF THE ISOVECTOR P WAVE OF $\pi\pi$ SCATTERING

As we already noted, the results obtained in the analysis of the isovector-P-wave $\pi\pi$-scattering data [65–67], using both the 2-channel model-independent method and the 5-channel Breit-Wigner one [32,57], require further inves-

tigation. Though conclusions in both methods mainly confirm each other, one can see advantages of the former in the description of data in comparison with the latter. Therefore, we further apply the model-independent method in which we consider the cases with four [$\rho(770)$, $\rho(1250)$, $\rho(1600)$, and $\rho(1800)$] and five [adding $\rho(1450)$] resonances, allowing for the results of our previous works [32,57]. In [57], we discussed in detail our selection of the used experimental data [65–67]. There it is noted that comparing the data [66] with that of Refs. [65,67], one can see that the points of the phase shifts δ of the former lie systematically by 1°–5° higher than the ones of the latter, except for two points of Ref. [65] at 710 and 730 MeV, which lie by about 2° higher than the corresponding points of Ref. [66] (these points are omitted in the subsequent analysis). Therefore, we have supposed a constant systematic error that must be determined in the combined analysis of data, i.e., should be considered as a fitted parameter. This simple assumption, which is the least offensive intervention to the data because it does not change their character, made the used data mutually consistent. To reduce influence of the background on obtained parameters of resonances, we perform the analysis of the data in the 3-channel approach taking into account a threshold of the third effective channel in the corresponding uniformizing variable of type (5). Of course, we do not know in advance the position of the threshold of this third channel, though, considering the experimental data [65–67], one might suppose that it lies in the region of 1500 MeV. From fitting to the data we obtained $\sqrt{s_3} \approx 1512.35$ MeV and interpret this channel as $\rho\sigma$. The influence of other channels which couple to the $\pi\pi$ one was supposed to be taken into account via the background. As a result of analysis, it turned out that this influence is negligible for the considered data, except for a not-large suppression of the S-matrix element module related to some combined influence of both the crossed and coupled channels which open below 1500 MeV (the only parameter). Furthermore, we make a constant shift in the phase of the amplitude, which does not concern the influence of other channels and is a technical detail of our approximation related to the neglect of the $\pi\pi$-threshold branch point. Since a value of the indicated shift is found in fitting to data, we include it among the fitted parameters.

So, in $S_{\rm res}$, $d_{\rm res}$ is taken in the form (9). In the analysis, we obtained that a description is improved a little if we take into account in the uniformizing variable (5) the branch point related to the threshold of the $\rho 2\pi$ channel instead of the near $\omega\pi^0$ one, as was done in [32,57], i.e., $s_2 = (m_\rho + 2m_{\pi^0})^2$. For the background part S_B, the d function has the following form, as the result of analysis:

$$d_B = \exp\left[-ia\,\mathrm{sgn}(k_1) + \left(\frac{k_1}{m_{\pi^+}}\right)^3 b\right], \qquad (12)$$

where $k_1 = \sqrt{s - s_1}/2$, $s_1 = 4m^2_{\pi^+}$, and a and b are real numbers.

First we present the results of the analysis with four resonances. It turns out that the $\rho(770)$ and $\rho(1250)$ are described by the pole clusters of types (a) and (e), respectively, whereas other ρ-like mesons [$\rho(1600)$ and $\rho(1800)$] are represented by the clusters of types (b) or (c) in various combinations (see Table I). Even if a quality of description of the data (χ^2) is practically the same for various possible scenarios the obtained parameters of resonances (mainly the widths) differ considerably (see Table I).

Masses and total widths in Table I have been calculated from the pole positions on sheets II, IV, and VIII for resonances of types (a), (b) [and (e)], and (c), respectively, because, as one can see in Refs. [9,40], the analytic continuations of the corresponding S-matrix elements only on these sheets have the forms $\propto 1/S^{\rm I}_{11}$, $\propto 1/S^{\rm I}_{22}$, and $\propto 1/S^{\rm I}_{33}$, respectively, ($S^{\rm I}_{aa}$ is the S-matrix element on the physical sheet), i.e., the pole positions of resonances only on these sheets are at the same points of the complex-energy plane, as the resonance zeros on the physical sheet, and are not shifted due to the coupling of channels. When calculating the masses and total widths, the resonance part of the amplitude is taken in the form

$$T^{\rm res} = \frac{\sqrt{s}\Gamma_{\rm el}}{m^2_{\rm res} - s - i\sqrt{s}\Gamma_{\rm tot}}. \qquad (13)$$

If the pole position is $\sqrt{s_r} = \mathrm{E}_r - i\Gamma_r/2$, then

$$m_{\rm res} = \sqrt{\mathrm{E}_r^2 + \left(\frac{\Gamma_r}{2}\right)^2} \quad \text{and} \quad \Gamma_{\rm tot} = \Gamma_r. \qquad (14)$$

TABLE I. The masses and total widths (in MeV) of vector resonances, obtained at analyzing only the $\pi\pi$ scattering, for various acceptable variants of representation of the four states considered. The letters in the first column denote the pole clusters describing, respectively, resonances $\rho(770)$, $\rho(1250)$, $\rho(1600)$, and $\rho(1800)$. "NDF" denotes a number of degrees of freedom.

	χ^2/NDF	$\rho(770)$		$\rho(1250)$		$\rho(1600)$		$\rho(1800)$	
		$m_{\rm res}$	$\Gamma_{\rm tot}$	$m_{\rm res}$	$\Gamma_{\rm tot}$	$m_{\rm res}$	$\Gamma_{\rm tot}$	$m_{\rm res}$	$\Gamma_{\rm tot}$
aebb	1.73	769.7	145.5	1292.6	252.6	1593.6	117.6	1789.7	155.6
aebc	1.72	769.8	144.9	1317.2	332.3	1595.3	128.4	1787.2	197.6
aecb	1.74	769.8	144.7	1275.5	357.6	1594.3	81.8	1792.0	132.6
aecc	1.71	769.6	145.1	1292.5	315.9	1596.2	70.8	1789.6	162.8

Though a relevant scenario from the ones, indicated in Table I, can be selected only by performing the combined analysis of several coupled processes, let us present the formally best scenario in more detail. It is when the $\rho(770)$, $\rho(1250)$, $\rho(1600)$, and $\rho(1800)$ are represented by the pole clusters of types (a), (e), (c), and (c), respectively. In this case the total χ^2/NDF equals $276.895/(183-21)=1.71$ and the indicated systematic error of data [66] is $-1.876^\circ \pm 0.144^\circ$. The background parameters are $a=-0.2851\pm0.0016$ and $b=0.000\,11\pm0.000\,04$; $\sqrt{s_3}=1512.35\pm3.9$ MeV. When calculating χ^2 for the inelasticity parameter $\eta=|S_{\pi\pi\to\pi\pi}|$, three points of data [67] at 990, 1250, and 1825 MeV have been omitted as giving the anomalously big contribution to χ^2. When calculating χ^2 for the phase shift δ, three points of data [66] have been omitted in all four cases: the one at 790 MeV from the s-channel analysis, and two at 790 and 850 MeV from the t-channel one. The obtained zero positions, on the w plane, of the corresponding resonances are as follows:

for $\rho(770)$:

$$w_1 = 0.109\,261 + 1.882\,213i,$$
$$w_2 = -0.030\,737 + 0.529\,505i,$$
$$w_3 = -0.109\,261 - 1.882\,213i,$$
$$w_4 = 0.030\,737 - 0.529\,505i,$$

for $\rho(1250)$:

$$w_{21} = 0.482\,066 + 0.539\,05i,$$
$$w_{22} = -0.492\,996 + 0.549\,948i,$$
$$w_{23} = w_{24} = -0.740\,431 - 1.165\,967i,$$
$$w_{25} = w_{26} = 0.922\,579 - 1.047\,898i,$$
$$w_{27} = -0.578\,074 - 0.413\,197i,$$
$$w_{28} = 0.562\,951 - 0.408\,265i,$$

for $\rho(1600)$:

$$w_9 = -1.596\,824 - 0.217\,455i,$$
$$w_{10} = 1.584\,821 - 0.143\,875i,$$
$$w_{11} = -0.625\,828 - 0.056\,814i,$$
$$w_{12} = 0.614\,841 - 0.083\,729i,$$

for $\rho(1800)$:

$$\tilde{w}_9 = -2.232\,385 - 0.357\,44i,$$
$$\tilde{w}_{10} = 2.252\,998 - 0.513\,244i,$$
$$\tilde{w}_{11} = -0.445\,442 - 0.046\,662i,$$
$$\tilde{w}_{12} = 0.451\,545 - 0.014\,187i.$$

In Table II, we show the pole clusters of these ρ-like states [not considering the $\rho(1450)$] on the lower $\sqrt{s}$-half-plane (in MeV) (the conjugate poles on the upper half-plane are not shown). When fitting to the data, we generated simple poles by using the simplest Breit-Wigner forms to diminish the number of fitted parameters. This explains the equality of errors of a number of the real and imaginary parts of pole positions on various sheets because these errors are calculated from the obtained ones for the generator parameters. This concerns both the vector sector and the scalar one considered further in Sec. IV.

In the case of five resonances, $\rho(770)$, $\rho(1250)$, $\rho(1450)$, $\rho(1600)$, and $\rho(1800)$, we obtain some more (in comparison with the previous case) possible scenarios [with the representation of resonances $\rho(1450)$, $\rho(1600)$, and $\rho(1800)$ by various pole clusters] which give the same satisfactory description of the process. However, parameters of resonances (mainly the widths) differ considerably. In Table III, we show the quality of description in these scenarios and obtained parameters of resonances. Considering Tables I and III, one can conclude that it is impossible to obtain reliable information on the multichannel resonances analyzing only one process even in the vector sector. This statement holds still more for such broad resonances as the scalar ones.

TABLE II. The pole clusters distributed on sheets II–VIII for the case with four resonances of the ρ family. $\sqrt{s_r}=\mathrm{E}_r-i\Gamma_r/2$ in MeV is given.

Sheet		II	III	IV	V	VI	VII	VIII
$\rho(770)$	E_r	766.18 ± 0.29	766.18 ± 0.29			766.18 ± 0.29	766.18 ± 0.29	
	$\Gamma_r/2$	72.55 ± 0.28	72.55 ± 0.28			72.55 ± 0.28	72.55 ± 0.28	
$\rho(1250)$	E_r		1282.8 ± 51.4	1282.8 ± 51.4	1278.8 ± 1	1191.8 ± 1.1	1399.2 ± 51.4	1399.2 ± 51.4
	$\Gamma_r/2$		146.45 ± 19.3	157.95 ± 19.3	163.5 ± 2.6	154.2 ± 2.2	157.95 ± 19.3	146.45 ± 19.3
$\rho(1600)$	E_r				1595.8 ± 5.6	1595.8 ± 5.6	1595.8 ± 5.6	1595.8 ± 5.6
	$\Gamma_r/2$				35.4 ± 4.4	54.4 ± 4.4	54.4 ± 4.4	35.4 ± 4.4
$\rho(1800)$	E_r				1787.7 ± 13.8	1787.7 ± 13.8	1787.7 ± 13.8	1787.7 ± 13.8
	$\Gamma_r/2$				183.2 ± 16.2	126.0 ± 16.2	24.2 ± 16.2	81.4 ± 16.2

TABLE III. The masses and total widths (in MeV) of vector resonances, obtained at analyzing only the $\pi\pi$ scattering, for various acceptable variants of representation of the five states considered. The letters in the first column denote the pole clusters describing, respectively, resonances $\rho(770)$, $\rho(1250)$, $\rho(1450)$, $\rho(1600)$, and $\rho(1800)$.

	χ^2/NDF	$\rho(770)$		$\rho(1250)$		$\rho(1450)$		$\rho(1600)$		$\rho(1800)$	
		$m_{\rm res}$	$\Gamma_{\rm tot}$	$m_{\rm res}$	$\Gamma_{\rm tot}$	$m_{\rm res}$	$\Gamma_{\rm tot}$	$m_{\rm res}$	$\Gamma_{\rm tot}$	$m_{\rm res}$	$\Gamma_{\rm tot}$
aebbb	1.77	769.7	144.7	1264.9	252.3	1429.9	231.4	1593.7	117.6	1790.2	156.4
aebbc	1.76	769.8	144.9	1274.7	304.3	1429.7	232.7	1595.3	128.5	1787.1	197.4
aebcb	1.77	769.7	144.7	1247.4	303.3	1441.8	228.8	1595.7	74.0	1779.6	153.7
aecbb	1.76	769.8	145.4	1303.3	242.5	1465.5	260.8	1595.9	134.0	1777.5	67.1
aebcc	1.77	769.6	144.8	1251.9	315.1	1442.0	229.2	1596.2	70.8	1786.4	176.0
aecbc	1.77	769.8	145.3	1312.6	317.0	1468.6	166.8	1593.9	128.8	1780.8	217.0
aeccb	1.77	769.8	144.9	1276.4	307.1	1466.0	259.8	1595.1	81.8	1785.8	104.2
aeccc	1.76	769.7	144.8	1273.0	168.3	1481.6	139.7	1596.2	73.0	1782.2	79.1

From consideration of Tables I and III, one can see that the description with four resonances is a little better than with five resonances. However, we prefer to speak about the five-resonance description of data on the isovector P wave of $\pi\pi$ scattering below 1880 MeV, because, as discussed in the Introduction and in [32,57], there are possible experimental indications for the SU(3) partners of the $\rho(1450)$ if the $\rho(1450)$ is considered as the $^3D_1$ $q\bar{q}$ state.

Let us describe also in this case the formally best scenario in more detail. It is when the $\rho(770)$, $\rho(1250)$, $\rho(1450)$, $\rho(1600)$, and $\rho(1800)$ are represented by the pole clusters of types (a), (e), (b), (b), and (c), respectively. Here the total χ^2/NDF equals $278.055/(183-25) = 1.76$ and the above-discussed systematic error of data [66] is $-1.858° \pm 0.144°$. The background parameters are $a = -0.2819 \pm 0.0016$ and $b = 0.000\,109 \pm 0.000\,04$; $\sqrt{s_3} = 1512.35 \pm 4.82$ MeV. When calculating the total χ^2, the same experimental points, as in the 4-resonance case, have been omitted as giving the anomalously big contribution to χ^2. The obtained zero positions, on the w plane, of the considered resonances are as follows:

for $\rho(770)$:

$$w_1 = 0.109\,126\,4 + 1.881\,929\,4i,$$
$$w_2 = -0.030\,709 + 0.529\,588\,8i,$$
$$w_3 = -0.109\,126\,4 - 1.881\,929\,4i,$$
$$w_4 = 0.030\,709 - 0.529\,588\,8i,$$

for $\rho(1250)$:

$$w_{21} = 0.470\,730\,6 + 0.560\,244\,7i,$$
$$w_{22} = -0.487\,058\,8 + 0.578\,878\,6i,$$
$$w_{23} = w_{24} = -0.714\,041\,8 - 1.140\,278\,7i,$$
$$w_{25} = w_{26} = 0.896\,537 - 0.986\,369\,5i,$$
$$w_{27} = -0.582\,327\,5 - 0.451\,324\,2i,$$
$$w_{28} = 0.558\,892\,2 - 0.440\,869\,6i,$$

for $\rho(1450)$:

$$w_5 = 0.632\,819\,6 + 0.386\,632\,1i,$$
$$w_6 = -0.654\,016 + 0.390\,975\,9i,$$
$$w_7 = -1.267\,791\,2 - 0.564\,149\,4i,$$
$$w_8 = 1.291\,685\,9 - 0.599\,597\,2i,$$

for $\rho(1600)$:

$$\tilde{w}_5 = 0.610\,283\,3 + 0.097\,674\,3i,$$
$$\tilde{w}_6 = -0.625\,873\,1 + 0.065\,265\,8i,$$
$$\tilde{w}_7 = -1.597\,658\,9 - 0.255\,701\,3i,$$
$$\tilde{w}_8 = 1.580\,580\,4 - 0.164\,822\,2i,$$

for $\rho(1800)$:

$$w_9 = -2.221\,654 - 0.344\,303\,8i,$$
$$w_{10} = 2.242\,002 - 0.500\,348\,9i,$$
$$w_{11} = -0.444\,182\,8 - 0.056\,578\,4i,$$
$$w_{12} = 0.452\,262\,6 - 0.024\,626\,5i.$$

In Table IV, we show the pole clusters of the ρ-like states [considering the $\rho(1450)$] on the lower $\sqrt{s}$-half-plane (the conjugate poles on the upper half-plane are not shown).

Note that in Tables II and IV, the shown pole positions of the pole cluster on all the appropriate sheets, which describes the $\rho(770)$, are at the same point of the complex-energy plane $\sqrt{s}$, i.e., the poles on the various sheets are not shifted one with respect to another by channel couplings due to the $\rho(770)$. This means that the state $\rho(770)$ has turned out to be elastic in the accuracy level of the analyzed data, though earlier at the Breit-Wigner description of the same data [32,57], we found a considerable coupling of the $\rho(770)$ with the four-pion channels. However, the Breit-Wigner approach is less satisfactory than the model-independent one, when describing all data up to 1880 MeV. It seems that taking into account explicitly the $(\pi\pi)(\pi\pi)$-threshold branch point in the corresponding

TABLE IV. Pole clusters distributed on sheets II–VIII for the case with five resonances of the ρ family. $\sqrt{s_r} = \mathrm{E}_r - i\Gamma_r/2$ in MeV is given.

Sheet		II	III	IV	V	VI	VII	VIII
$\rho(770)$	E_r	766.35 ± 0.3	766.35 ± 0.3			766.35 ± 0.3	766.35 ± 0.3	
	$\Gamma_r/2$	72.43 ± 0.28	72.43 ± 0.28			72.43 ± 0.28	72.43 ± 0.28	
$\rho(1250)$	E_r		1265.6 ± 32.6	1265.6 ± 32.6	1286.0 ± 1.0	1190.3 ± 1.1	1375.8 ± 32.6	1375.8 ± 32.6
	$\Gamma_r/2$		134.2 ± 11.8	152.2 ± 11.8	137.9 ± 2.45	139.5 ± 2.2	152.2 ± 11.8	134.2 ± 11.8
$\rho(1450)$	E_r		1425.1 ± 26.3	1425.1 ± 26.3	1480.3 ± 26.3	1480.3 ± 26.3		
	$\Gamma_r/2$		103.6 ± 24.3	116.2 ± 24.3	116.2 ± 24.3	103.6 ± 24.3		
$\rho(1600)$	E_r		1594.0 ± 5.4	1594.0 ± 5.4	1594.0 ± 5.4	1594.0 ± 5.4		
	$\Gamma_r/2$		40.45 ± 3.9	64.25 ± 3.9	40.45 ± 3.9	64.25 ± 3.9		
$\rho(1800)$	E_r				1784.4 ± 13.7	1784.4 ± 13.7	1784.4 ± 13.7	1784.4 ± 13.7
	$\Gamma_r/2$				177.9 ± 16.2	120.9 ± 16.2	41.7 ± 16.2	98.7 ± 16.2

uniformizing variable in the 3-channel approach, one will obtain some shift of poles of this cluster due to the coupling of the $\rho(770)$ with the four-pion channels.

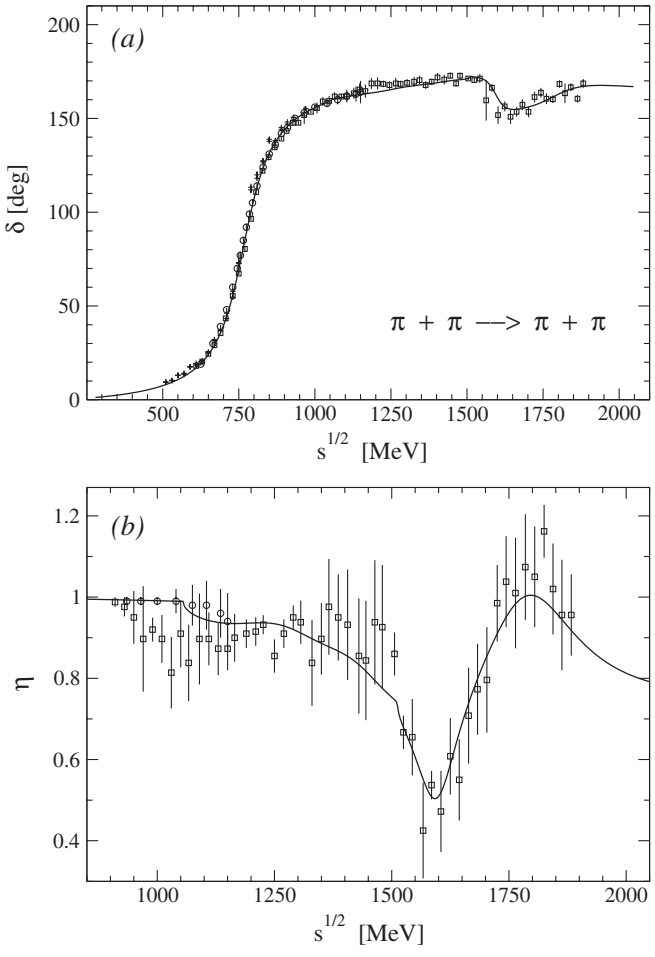

FIG. 2. The phase shift δ of amplitude and module η of the S-matrix element for the P-wave $\pi\pi$ scattering. The data are from Refs. [65] (circle), [66] (plus), and [67] (square).

In Fig. 2 we present results of fitting to the data with five resonances.

IV. ANALYSIS OF THE ISOSCALAR-SCALAR SECTOR

Considering the S waves of processes $\pi\pi \to \pi\pi$, $K\bar{K}$, $\eta\eta$, and $\eta\eta'$ in the model-independent method, we performed two variants of the 3-channel analysis of the data [67–69,43,44][3]:

variant I: the combined analysis of $\pi\pi \to \pi\pi$, $K\bar{K}$, and $\eta\eta$;

variant II: the analysis of $\pi\pi \to \pi\pi$, $K\bar{K}$, and $\eta\eta'$.

Influence of the $\eta\eta'$ channel in variant I and the $\eta\eta$ channel in variant II is taken into account via the background. Here, the left-hand cuts are neglected in the Riemann-surface structure assuming that contributions on these cuts are also included in the background.

In this case, the subscripts in the matrix elements S_{ab} denote a, b = 1-$\pi\pi$, 2-$K\bar{K}$, 3-$\eta\eta$, or $\eta\eta'$. In the uniformizing variable (5), $s_2 = 4m_K^2$, and $s_3 = 4m_\eta^2$ or $(m_\eta + m_{\eta'})^2$ in variants I or II, respectively.

The S-matrix elements in relations (6) are taken as the products (8) where the resonance part d_{res} has the form (9) and the background part is

$$d_B = \exp\Big[-i\sum_{n=1}^{3}\frac{k_n}{m_n}(\alpha_n + i\beta_n)\Big], \qquad (15)$$

with

[3]Note that there are alternative data, e.g., one of the solutions of the phase analysis in Ref. [75] and the recent phase analysis in Ref. [76] which are in accordance with each other, but which differ from those used here, especially in the energy region of $f_0(980)$. Analysis with these data should be performed separately. This work is in progress.

$$\alpha_n = a_{n1} + a_{n\sigma}\frac{s-s_\sigma}{s_\sigma}\theta(s-s_\sigma) + a_{nv}\frac{s-s_v}{s_v}\theta(s-s_v), \tag{16}$$

$$\beta_n = b_{n1} + b_{n\sigma}\frac{s-s_\sigma}{s_\sigma}\theta(s-s_\sigma) + b_{nv}\frac{s-s_v}{s_v}\theta(s-s_v), \tag{17}$$

where s_σ is the $\sigma\sigma$ threshold and s_v is a combined threshold of many opened channels in the vicinity of 1.5 GeV (e.g., $\eta\eta'$, $\rho\rho$, and $\omega\omega$). These thresholds are determined in the analysis.

In variant II, the terms

$$a'_{n\eta}\frac{s-4m_\eta^2}{4m_\eta^2}\theta(s-4m_\eta^2) \quad \text{and} \quad b'_{n\eta}\frac{s-4m_\eta^2}{4m_\eta^2}\theta(s-4m_\eta^2) \tag{18}$$

should be added to α'_n and β'_n to account for an influence of the $\eta\eta$ channel (here and in the following, the quantities related to variant II are primed).

When analyzing the data in the scalar sector, we included all the five resonances discussed below 1.9 GeV in the PDG issue [1] including the $f_0(1370)$. As to the latter, we said already in the Introduction that there are definite doubts if it exists or not as a single resonance [7,33]. However, Bugg [34] gave serious arguments in favor of its existence. In this paper we take a more standard point of view that this state exists [1], the more so, as it was shown [10,32]; the $f_0(1370)$ (if it exists) should have the dominant $s\bar{s}$ component and might be put to a nonet with the $f_0(600)$, the isovector $a_0(980)$, and the isodoublet $K_0^*(900)$.

In the analysis we got a satisfactory description in both variants; moreover, due to the combined consideration of several processes, we removed an arbitrariness in the representation of multichannel resonances, which is demonstrated in the previous section as to the vector mesons. Therefore, the results, obtained here for scalar mesons, are rather decisive.

In variant I, we have the following description: for the $\pi\pi$ scattering, $\chi^2/\mathrm{NDF} \approx 1.25$; for $\pi\pi \to K\bar{K}$, $\chi^2/\mathrm{NDF} \approx 1.68$; for $\pi\pi \to \eta\eta$, $\chi^2/\mathrm{N.exp.points} \approx 0.78$. The total χ^2/NDF is $325.924/(301-39) \approx 1.24$. From possible resonance representations by pole clusters, the analysis selects the following one: the $f_0(600)$ is described by the cluster of type (a); $f_0(1370)$, type (c); $f_0(1500)$, type (g); $f_0(1710)$, type (c); and the $f_0(980)$ is represented only by the pole on sheet II and shifted pole on sheet III in both variants. In Table V we indicate the obtained pole clusters for resonances on the eight sheets of the Riemann surface on which the 3-channel S matrix is determined. The poles on sheets IV, VI, VIII, and V, corresponding to the $f_0(1500)$, are of the 2nd and 3rd orders, respectively (this is an approximation). The background parameters are $a_{11} = 0.2071$, $a_{1\sigma} = 0.0088$, $a_{1v} = 0$, $b_{11} = b_{1\sigma} = 0$, $b_{1v} = 0.0495$, $a_{21} = -0.2722$, $a_{2\sigma} = -0.9137$, $a_{2v} = -5.64$, $b_{21} = 0.0969$, $b_{2\sigma} = 0$, $b_{2v} = 7.075$, $b_{31} = 0.711$, $b_{3\sigma} = 0.574$, and $b_{3v} = 0$; $s_\sigma = 1.638\ \mathrm{GeV}^2$, $s_v = 2.084\ \mathrm{GeV}^2$. When calculating χ^2, the following experimental points have been omitted as giving the anomalously large contribution to χ^2: from the $\pi\pi$ scattering data the points at 525, 730, and 990 MeV for the phase shift δ_{11} and the points at 990, 1650, and 1850 MeV for $\eta_{11} = |S_{11}|$, from the $\pi\pi \to K\bar{K}$ data the points at 1073, 1082, and 1387 MeV for the phase shift ϕ_{12}, and the points at 1002, 1208.9, and 1235.7 MeV for the $\eta_{12} = |S_{12}|$. The obtained zero positions, on the w plane, of the resonances are as follows:

for $f_0(600)$:

$$w_1 = 1.215\,56 + 4.348\,551\,5i,$$
$$w_2 = -0.057\,805\,8 + 0.213\,175\,8i,$$
$$w_3 = -0.993\,171\,4 - 4.498\,227\,8i,$$
$$w_4 = 0.048\,382\,8 - 0.212\,194\,6i,$$

TABLE V. The pole clusters for the f_0 resonances in variant I. $\sqrt{s_r} = \mathrm{E}_r - i\Gamma_r/2$ in MeV is given.

Sheet		II	III	IV	V	VI	VII	VIII
$f_0(600)$	E_r	596.1 ± 13	583.9 ± 14			503.9 ± 13	516.1 ± 14	
	$\Gamma_r/2$	494 ± 18	494 ± 18			494 ± 18	494 ± 18	
$f_0(980)$	E_r	1009 ± 4	974.5 ± 9					
	$\Gamma_r/2$	34.3 ± 4.9	57.3 ± 6					
$f_0(1370)$	E_r				1398.3 ± 16	1398.3 ± 16	1398.3 ± 16	1398.3 ± 16
	$\Gamma_r/2$				287.5 ± 17	270.5 ± 17	155.1 ± 17	172.1 ± 17
$f_0(1500)$	E_r	1502.6 ± 16	1479.6 ± 13	1502.6 ± 16	1496.7 ± 15	1500 ± 16	1502 ± 12	1502.6 ± 16
	$\Gamma_r/2$	357.2 ± 18	135.5 ± 12	238.8 ± 18	140.2 ± 13	190.7 ± 15	87.7 ± 11	356.6 ± 18
$f_0(1710)$	E_r				1708 ± 13	1708 ± 13	1708 ± 13	1708 ± 13
	$\Gamma_r/2$				138.6 ± 14	113.2 ± 14	86 ± 14	111.4 ± 14

for $f_0(980)$:

$$\tilde{w}_1 = 0.691\,689\,8 + 1.214\,342\,3i,$$
$$\tilde{w}_2 = -0.209\,760\,1 + 0.518\,978\,7i,$$

for $f_0(1370)$:

$$w_9 = -4.113\,826\,4 - 1.650\,733\,3i,$$
$$w_{10} = 4.132\,813\,7 - 1.746\,201\,6i,$$
$$w_{11} = -0.232\,326\,7 - 0.062\,298\,1i,$$
$$w_{12} = 0.235\,934\,6 - 0.057\,427\,8i,$$

for $f_0(1500)$:

$$w_{29} = 4.767\,463\,7 + 2.018\,836\,6i,$$
$$w_{30} = 0.196\,978\,6 + 0.058\,143\,1i,$$
$$w_{31} = w_{32} = -0.216\,554 + 0.038\,948i,$$
$$w_{33} = w_{34} = w_{35} = -4.622\,36 - 1.110\,35i,$$
$$w_{36} = w_{37} = 4.575\,409\,1 - 0.823\,079i,$$
$$w_{38} = -0.177\,959\,8 - 0.075\,249\,6i,$$
$$w_{39} = w_{40} = 0.215\,419\,2 - 0.024\,234\,6i,$$

for $f_0(1710)$:

$$\tilde{w}_9 = -5.734\,040\,2 - 0.604\,359\,8i,$$
$$\tilde{w}_{10} = 5.739\,894\,8 - 0.739\,202\,3i,$$
$$\tilde{w}_{11} = -0.172\,551\,6 - 0.017\,899\,8i,$$
$$\tilde{w}_{12} = 0.173\,433\,9 - 0.013\,911\,9i.$$

In variant II, we get the following description: for the $\pi\pi$ scattering $\chi^2/\mathrm{NDF} \approx 1.0$; for $\pi\pi \to K\bar{K}$, $\chi^2/\mathrm{NDF} \approx 1.64$; for $\pi\pi \to \eta\eta'$, $\chi^2/\mathrm{N.exp.points} \approx 0.35$. The total χ^2/NDF is $283.782/(293 - 38) \approx 1.11$. When calculating χ^2, the following experimental points have been omitted as giving the anomalously big contribution to χ^2: from the $\pi\pi$ scattering data the same points as in variant I, from the $\pi\pi \to K\bar{K}$ data the points at 1073, 1383, and 1387 MeV for the phase shift ϕ_{12} and the points at 1002, 1264.9, and 1286.9 MeV for the η_{12}. In this case, the $f_0(600)$ is described by the cluster of type (a′); $f_0(1370)$, type (b′); $f_0(1500)$, type (d′); and $f_0(1710)$, type (c′). In Table VI we indicate the obtained pole clusters for resonances on the eight sheets of the Riemann surface. The poles on sheets IV and V, corresponding to the $f_0(1500)$, are of 2nd order (this is an approximation). The background parameters are $a'_{11} = 0.0124$, $a'_{1\eta} = -0.0606$, $a'_{1\sigma} = 0$, $a'_{1v} = 0.1004$, $b'_{11} = b'_{1\eta} = b'_{1\sigma} = 0$, $b'_{1v} = 0.0469$, $a'_{21} = -3.4335$, $a'_{2\eta} = -0.5008$, $a'_{2\sigma} = 1.7364$, $a'_{2v} = -5.366$, $b'_{21} = 0$, $b'_{2\eta} = -0.7383$, $b'_{2\sigma} = 2.6772$, $b'_{2v} = 1.903$, $b'_{31} = 0.5511$, $s_\sigma = 1.638\ \mathrm{GeV}^2$, and $s_v = 2.126\ \mathrm{GeV}^2$. The obtained zero positions, on the w' plane, of the resonances are as follows:

for $f_0(600)$:

$$w'_1 = 0.498\,958\,7 + 2.206\,977\,9i,$$
$$w'_2 = -0.098\,655\,5 + 0.431\,242\,8i,$$
$$w'_3 = -0.481\,454\,9 - 2.218\,535\,9i,$$
$$w'_4 = 0.092\,263\,7 - 0.430\,293\,4i,$$

for $f_0(980)$:

$$\tilde{w}'_1 = 0.238\,743\,6 + 1.098\,388\,7i,$$
$$\tilde{w}'_2 = -0.160\,039\,2 + 0.786\,601\,8i,$$

for $f_0(1370)$:

$$w'_5 = 0.496\,496\,8 + 0.374\,192\,2i,$$
$$w'_6 = -0.512\,511\,8 + 0.378\,453\,3i,$$
$$w'_7 = -1.301\,409\,8 - 0.908\,727\,5i,$$
$$w'_8 = 1.323\,011\,6 - 0.945\,256\,9i,$$

TABLE VI. The pole clusters for the f_0 resonances in variant II. $\sqrt{s'_r} = \mathrm{E}'_r - i\Gamma'_r/2$ in MeV is given.

Sheet		II	III	IV	V	VI	VII	VIII
$f_0(600)$	E'_r	616.5 ± 8	621.8 ± 10			598.3 ± 8	593 ± 10	
	$\Gamma'_r/2$	554 ± 11	554 ± 11			554 ± 11	554 ± 11	
$f_0(980)$	E'_r	1009.2 ± 3.5	985.8 ± 5.7					
	$\Gamma'_r/2$	31.3 ± 4.7	58 ± 5.5					
$f_0(1370)$	E'_r		1394.4 ± 9	1394.4 ± 9	1412.8 ± 9	1412.8 ± 9		
	$\Gamma'_r/2$		227.4 ± 10	244.6 ± 10	244.6 ± 10	227.4 ± 10		
$f_0(1500)$	E'_r	1498.3 ± 11	1502.4 ± 13	1498.3 ± 11	1498.3 ± 11	1494.6 ± 10	1498.3 ± 11	
	$\Gamma'_r/2$	198.8 ± 12	236.8 ± 15	193 ± 12	198.8 ± 12	194 ± 8	193 ± 12	
$f_0(1710)$	E'_r				1726.1 ± 11	1726.1 ± 11	1726.1 ± 11	1726.1 ± 11
	$\Gamma'_r/2$				140.2 ± 9	111.6 ± 9	84.2 ± 9	112.8 ± 9

for $f_0(1500)$:

$$w'_{13} = 1.460\,306 + 0.735\,458\,3i,$$
$$w'_{14} = 0.552\,139\,7 + 0.274\,032\,2i,$$
$$w'_{15} = w'_{16} = -0.510\,115\,5 + 0.276\,865\,1i,$$
$$w'_{17} = w'_{18} = -1.445\,342\,2 - 0.728\,275\,2i,$$
$$w'_{19} = 1.460\,306 - 0.735\,458\,3i,$$
$$w'_{20} = 0.552\,139\,7 - 0.274\,032\,2i,$$

for $f_0(1710)$:

$$w'_{9} = -1.445\,342\,2 - 0.728\,275\,2i,$$
$$w'_{10} = 2.022\,293 - 0.392\,918\,9i,$$
$$w'_{11} = -0.484\,890\,2 - 0.076\,796\,3i,$$
$$w'_{12} = 0.492\,258\,5 - 0.058\,868\,1i.$$

In Figs. 3–5, we show the results of fitting to the experimental data in both variants. The fact that in variant II we obtain a better description of the processes $\pi\pi \to \pi\pi$, $K\bar{K}$ than in variant I tells of an importance of taking into account explicitly the $\eta\eta'$ threshold. However, in variant II, we encounter elements of some pseudobackground: these are the negative values of coefficients b's related to an inelastic part of the background. This means the increasing inelastic part of the background that implies a necessity to consider explicitly some physical phenomenon, e.g., the additional resonances or representation of resonances by other pole clusters and the consideration in the uniformizing variable of the other-channel thresholds. The latter is the case here: the negative sign of the quantity $b'_{2\eta} = -0.7383$ implies necessity of the explicit consideration of the $\eta\eta$-threshold branch point. Therefore, as to resonances lying below 1500 MeV, the more adequate description is variant I, whereas for the ones above 1500 MeV variant II.

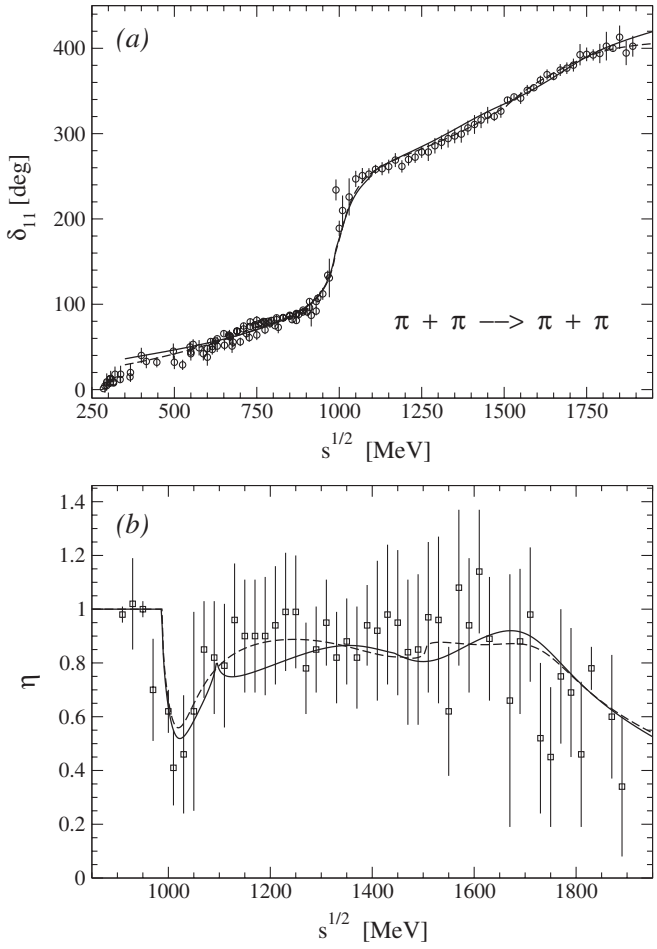

FIG. 3. The phase shift and module of the S-matrix element in the S-wave $\pi\pi$ scattering. The solid and dashed curves correspond to variants I and II, respectively. The data are from Refs. [65–68].

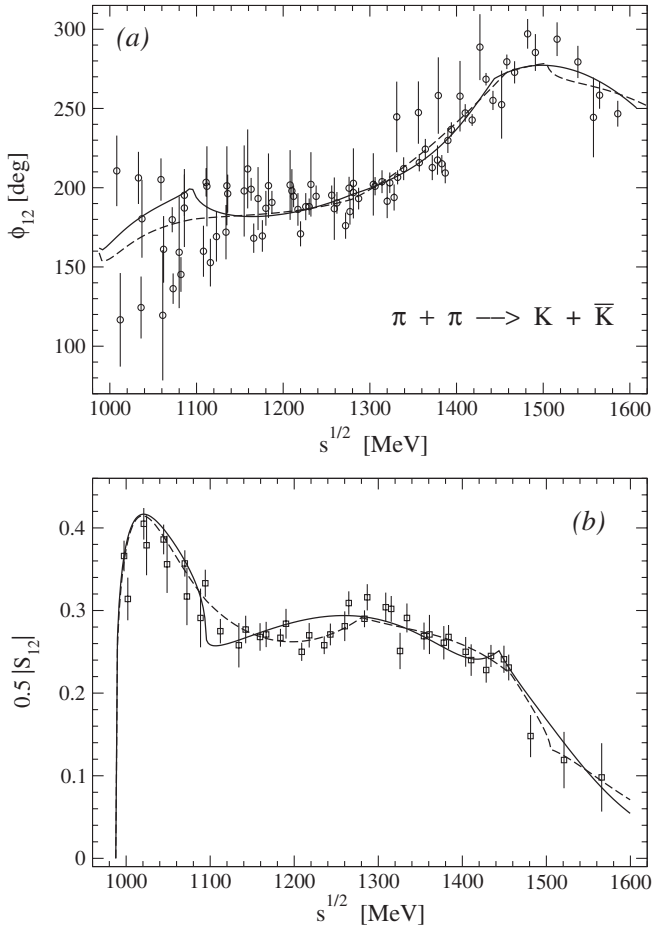

FIG. 4. The phase shift and module of the S-matrix element in the S wave of $\pi\pi \to K\bar{K}$. The solid and dashed curves correspond to variants I and II, respectively. The data are from Ref. [69].

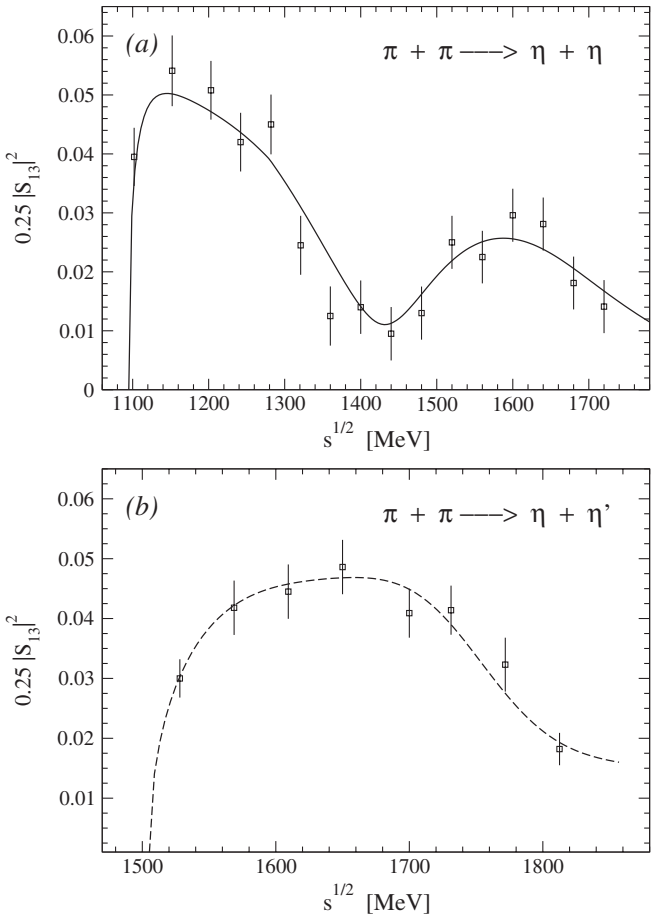

FIG. 5. The squared modules of the $\pi\pi \to \eta\eta$ (a) and $\pi\pi \to \eta\eta'$ (b) S-wave matrix elements. The data are from Refs. [43] (a) and from [44] (b).

Note also a benefit of comparison of results in both variants. As to the representation of the $f_0(600)$ and $f_0(980)$, both variants completely agree. Notice a surprising result obtained for the $f_0(980)$. This state lies slightly above the $K\bar{K}$ threshold and is described by the pole on sheet II and by the shifted pole on sheet III under the $\eta\eta$ threshold without the corresponding poles on sheets VI and VII, as it was expected for standard clusters. This may suggest that the $f_0(980)$ can be interpreted as the bound $\eta\eta$ state in accordance with the test discussed in Sec. II.

The $f_0(1370)$ is described by the cluster of type (c) in variant I and of type (b′) in variant II; this is reasonable taking into account the quark contents of the $K\bar{K}$ and $\eta\eta$ channels and the nearness of their thresholds and also if the representation of the $f_0(1370)$ by the (c) cluster in variant I did not presuppose a strong coupling of this state with some channel opening above the $\eta\eta$ one. Therefore, we tell about a dominant $s\bar{s}$ component of the $f_0(1370)$.

The $f_0(1500)$ is described by the cluster of type (g) in variant I and of type (d′) in variant II. The former indicates the approximately equal coupling constants of this state with the $\pi\pi$, $K\bar{K}$, and $\eta\eta$ systems, which apparently could point up to its glueball nature. The latter tells of the approximately equal coupling of this state with the $\pi\pi$ and $K\bar{K}$ channels, whereas the coupling with the $\eta\eta'$ channel is suppressed; these facts also point up to its glueball nature [19]. Therefore, we tell about a dominant glueball component in the wave function of the $f_0(1500)$.

Finally, the $f_0(1710)$ is described by the cluster of type (c) in variant I and of type (c′) in variant II. Taking into account the quark contents of the $\eta\eta'$ system, this could point up to the dominant $s\bar{s}$ component of this state.

Masses and total widths of states should be calculated from the pole positions, using the resonance part of amplitude in the form (13). Moreover, for resonances of types (a), (d), and (g), one ought to take the poles on sheets II, IV, and VIII, respectively [see a discussion of this point in Sec. III before Eq. (13)]. The obtained values of masses and total widths of the f_0 resonances are presented in Table VII.

Here let us note once more that multichannel states are most adequately represented by the pole clusters, i.e., by the poles on all corresponding sheets of the Riemann surface of the S matrix. The pole clusters give the main effect of resonances. The pole positions are rather stable characteristics for various models and they give an energy behavior of observed quantities, whereas masses and widths are very model dependent for wide resonances (see the discussion of this question in Refs. [7,57]). However, since at present in spectroscopy and in theoretical calculations the masses and total widths are used, we propose to apply the form (13) to the resonance part of amplitude (more accurately, the denominator of this expression) for determining masses and total widths from the pole positions. This form but with an additional form factor was used, e.g., in Ref. [77] at analyzing the $\pi\pi$ scattering in the isoscalar-scalar sector, though this form is inade-

TABLE VII. The masses and total widths of the f_0 resonances (all in MeV).

	Variant I		Variant II	
State	m_{res}	Γ_{tot}	m'_{res}	Γ'_{tot}
$f_0(600)$	774.2 ± 15.2	988 ± 36	828.8 ± 9.5	1108 ± 22
$f_0(980)$	1009.6 ± 4	68.6 ± 9.8	1009.7 ± 3.5	62.6 ± 9.4
$f_0(1370)$	1408.8 ± 16	344.2 ± 34	1415.7 ± 9	489.2 ± 20
$f_0(1500)$	1544.5 ± 16.1	714.4 ± 36	1511.4 ± 11	397.6 ± 24
$f_0(1710)$	1711.6 ± 13	222.8 ± 28	1729.8 ± 11	225.6 ± 18

quate already at the combined description of processes $\pi\pi \to \pi\pi$, $K\bar{K}$ above approximately 1200 MeV where a violation of the 2-channel unitarity becomes remarkable. In Ref. [78] one also used a similar formula at analyzing this sector and, in some analogy with introducing the form factor in Ref. [77], approximated the background S matrix by a ratio of polynomials of the second order.

V. ANALYSIS OF ISOSCALAR-TENSOR SECTOR

In analysis of the processes $\pi\pi \to \pi\pi$, $K\bar{K}$, and $\eta\eta$, we considered explicitly also the channel $(2\pi)(2\pi)$. Here it is impossible to use the uniformizing-variable method. Therefore, using the Le Couteur–Newton relations, we generate the resonance poles by some 4-channel Breit-Wigner forms. The $d(k_1, k_2, k_3, k_4)$ function is taken as $d = d_B d_{\rm res}$, where the resonance part is

$$d_{\rm res}(s) = \prod_r \Big[M_r^2 - s - i \sum_{j=1}^{4} \rho_{rj}^5 R_{rj} f_{rj}^2 \theta(s - 4m_j^2) \Big], \tag{19}$$

with $\rho_{rj} = 2k_j/\sqrt{M_r^2 - 4m_j^2}$ and f_{rj}^2/M_r the partial width, $j = 1, 2, 3$, and 4 denotes the $\pi\pi$, $(2\pi)(2\pi)$, $K\bar{K}$, and $\eta\eta$ channels, respectively. The Blatt-Weisskopf barrier factor for a tensor particle is

$$R_{rj} = \frac{9 + \frac{3}{4}(\sqrt{M_r^2 - 4m_j^2}\, r_{rj})^2 + \frac{1}{16}(\sqrt{M_r^2 - 4m_j^2}\, r_{rj})^4}{9 + \frac{3}{4}(\sqrt{s - 4m_j^2}\, r_{rj})^2 + \frac{1}{16}(\sqrt{s - 4m_j^2}\, r_{rj})^4}, \tag{20}$$

with radii of 0.943 fm for all resonances in all channels, except for $f_2(1270)$ and $f_2(1960)$ for which they are as follows: for $f_2(1270)$, 1.498, 0.708, and 0.606 fm in the channels $\pi\pi$, $K\bar{K}$, and $\eta\eta$, respectively; for $f_2(1960)$, 0.296 fm in the channel $K\bar{K}$, as a result of our analysis.

The background part has the form

$$d_B = \exp\Big[-i \sum_{n=1}^{3} \Big(\frac{2k_n}{\sqrt{s}} \Big)^5 (\alpha_n + i\beta_n) \Big] \tag{21}$$

with

$$\alpha_1 = a_{11} + \frac{s - 4m_K^2}{s} a_{12} \theta(s - 4m_K^2) + \frac{s - s_\upsilon}{s} a_{10} \theta(s - s_\upsilon), \tag{22}$$

$$\beta_n = b_n + \frac{s - s_\upsilon}{s} c_n \theta(s - s_\upsilon). \tag{23}$$

$s_\upsilon \approx 2.274$ GeV^2 is a combined threshold of the channels $\eta\eta'$, $\rho\rho$, and $\omega\omega$.

The data for the $\pi\pi$ scattering are taken from the energy-independent analysis by Hyams *et al.* [67]. Moreover, the first six experimental points for the inelasticity parameter η at 908, 930, 950, 970, 990, and 1010 MeV are excluded from our analysis because they settle down so as if in the 1000-MeV region there is some resonance. However, from general considerations, there should be no tensor meson here and the analyses of other processes also do not obtain any state of the f_2 family in this energetic region. Therefore, the $\pi\pi$ scattering in the tensor sector is assumed to be elastic from the threshold up to about 1130 MeV.

The data for $\pi\pi \to K\bar{K}$, $\eta\eta$ are taken from [70]. As the result of our analysis, the $K\bar{K}$ scattering is obtained to be elastic from the threshold up to 1200 MeV; the $\eta\eta$ scattering is almost elastic to about 1450 MeV.

We obtained a satisfactory description with ten resonances $f_2(1270)$, $f_2(1430)$, $f_2'(1525)$, $f_2(1580)$, $f_2(1730)$, $f_2(1810)$, $f_2(1960)$, $f_2(2000)$, $f_2(2240)$, and $f_2(2410)$ [the total $\chi^2/\mathrm{NDF} = 161.147/(168 - 65) \approx 1.56$] and with 11 states adding one more resonance $f_2(2020)$ which is needed in the combined analysis of processes $p\bar{p} \to \pi\pi$, $\eta\eta$, and $\eta\eta'$ [64]. In our analysis, the description with 11 resonances is practically the same as that with ten resonances: the total $\chi^2/\mathrm{NDF} = 156.617/(168 - 69) \approx 1.58$.

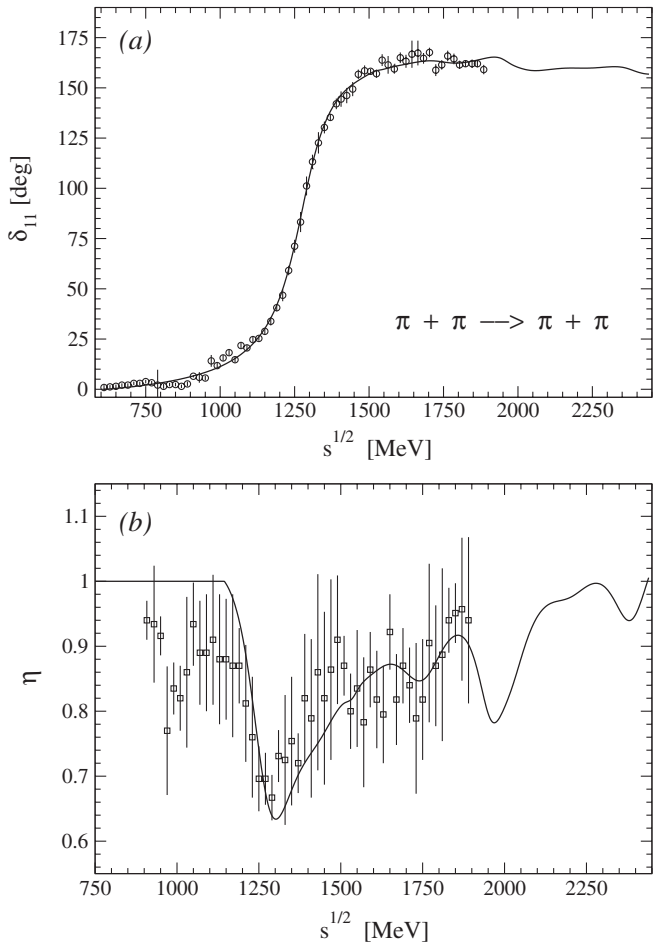

FIG. 6. The phase shift and module of the $\pi\pi$-scattering D-wave S-matrix element. The data are from Ref. [67].

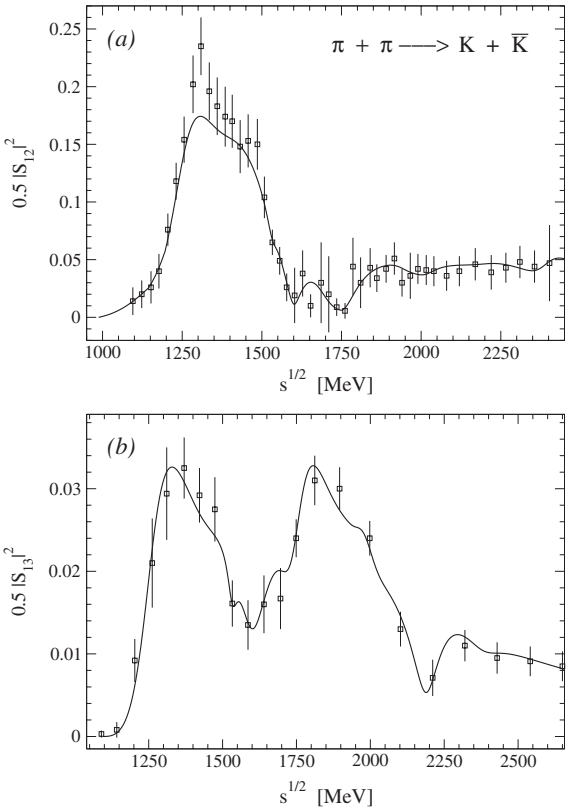

FIG. 7. The squared modules of the $\pi\pi \to K\bar{K}$ (a) and $\pi\pi \to \eta\eta$ (b) D-wave S-matrix elements. The data are from Ref. [70].

In Figs. 6 and 7 we show results of fitting to the data. When calculating χ^2 for the inelasticity parameter of the $\pi\pi$ scattering, three points of data [67] at 1070, 1310, and 1510 MeV have been omitted as giving the anomalously big contribution to χ^2; when calculating χ^2 for the phase shift δ_{11}, the points of data [67] at 970, 1544, and 1885 MeV have been omitted. By the same reason, when calculating χ^2 for the squared S-matrix element of process $\pi\pi \to K\bar{K}$, the points of data [70] at 1284, 1309, and 1653 MeV have been omitted.

The obtained resonance parameters are shown in Table VIII for the cases of 10 and 11 states. The background parameters for ten resonances are as follows: $a_{11} = -0.078\,05$, $a_{12} = 0.034\,45$, $a_{10} = -0.2295$, $b_1 = -0.0715$, $c_1 = -0.041\,65$, $b_2 = -0.981$, $c_2 = 0.736$, $b_3 = -0.5309$, $c_3 = 0.8223$; and for 11 resonances are as follows: $a_{11} = -0.0755$, $a_{12} = 0.0225$, $a_{10} = -0.2344$, $b_1 = -0.0782$, $c_1 = -0.052\,15$, $b_2 = -0.985$, $c_2 = 0.7494$, $b_3 = -0.5162$, and $c_3 = 0.786$.

We applied the Breit-Wigner forms (19) to generate the resonance poles on the 16-sheeted Riemann surface on which the 4-channel S matrix is determined. As we discussed in Sec. III, for determining parameters of resonances one should use only the poles lying on those sheets where the pole positions are at the same points of the complex-energy plane, as the resonance zeros on the physical sheet, i.e., they are not shifted due to the coupling of channels. Here these are sheets II, IV, VIII, and XVI to

TABLE VIII. The resonance parameters from the Breit-Wigner form (19) in the tensor sector for 10 and 11 states (in MeV).

State	M_r	f_{r1}	f_{r2}	f_{r3}	f_{r4}	$\approx \Gamma_{\text{tot}}$
			10 states			
$f_2(1270)$	1275.3 ± 1.8	470.8 ± 5.4	22.4 ± 4.6	201.5 ± 11.4	90.4 ± 4.76	211.8 ± 4.5
$f_2(1430)$	1450.8 ± 18.7	128.3 ± 45.9	8.2 ± 65	562.3 ± 142	32.7 ± 18.4	230.4 ± 17.1
$f_2'(1525)$	1535.0 ± 8.6	28.6 ± 8.3	41.6 ± 160	253.8 ± 78	92.6 ± 11.5	49.5 ± 20.7
$f_2(1565)$	1601.4 ± 27.5	75.5 ± 19.4	127 ± 199	315 ± 48.6	388.9 ± 27.7	169.7 ± 97.4
$f_2(1730)$	1723.4 ± 5.7	78.8 ± 43	107.6 ± 76.7	289.5 ± 62.4	460.3 ± 54.6	181.6 ± 45.2
$f_2(1810)$	1761.8 ± 15.3	129.5 ± 14.4	90.3 ± 90	259 ± 30.7	469.7 ± 22.5	176.7 ± 48.2
$f_2(1960)$	1962.8 ± 29.3	132.6 ± 22.4	65.4 ± 94	333 ± 61.3	319 ± 42.6	119 ± 27.3
$f_2(2000)$	2017 ± 21.6	143.5 ± 23.3	450.4 ± 221	614 ± 92.6	58.8 ± 24	299.0 ± 48.7
$f_2(2240)$	2207 ± 44.8	136.4 ± 32.2	166.8 ± 104	551 ± 149	375 ± 114	221.8 ± 68.8
$f_2(2410)$	2429 ± 31.6	177 ± 47.2	460.8 ± 209	411 ± 196.9	4.5 ± 70.8	169.5 ± 77.3
			11 states			
$f_2(1270)$	1276.3 ± 1.8	468.9 ± 5.5	7.2 ± 4.6	201.6 ± 11.6	89.9 ± 4.79	210.5 ± 4.4
$f_2(1430)$	1450.5 ± 18.8	128.3 ± 45.9	8.2 ± 63	562.3 ± 144	32.7 ± 18.6	230.1 ± 17.1
$f_2'(1525)$	1534.7 ± 8.6	28.5 ± 8.5	51.6 ± 155	253.9 ± 79	89.5 ± 12.5	49.5 ± 19.3
$f_2(1565)$	1601.5 ± 27.9	75.5 ± 19.6	127 ± 190	315 ± 50.6	388.9 ± 28.6	170.0 ± 93.4
$f_2(1730)$	1719.8 ± 6.2	78.8 ± 43	108.6 ± 76.0	289.5 ± 62.6	460.3 ± 54.5	182.4 ± 45.5
$f_2(1810)$	1760 ± 17.6	129.5 ± 14.8	90.3 ± 89.5	259 ± 32.0	469.7 ± 25.2	177.6 ± 48.5
$f_2(1960)$	1962.2 ± 29.8	132.6 ± 23.3	62.4 ± 91.3	331 ± 61.5	319 ± 42.8	118.6 ± 33.4
$f_2(2000)$	2006 ± 22.7	155.7 ± 24.4	574.8 ± 211	169.5 ± 95.3	60.4 ± 26.7	192.9 ± 56.4
$f_2(2020)$	2027 ± 25.6	50.4 ± 24.8	128 ± 190	441 ± 196.7	58 ± 50.8	106.9 ± 35.0
$f_2(2240)$	2202 ± 45.4	133.4 ± 32.6	168.8 ± 103	545 ± 150.4	381 ± 116	221.8 ± 71.7
$f_2(2410)$	2387 ± 33.3	175 ± 48.3	462.8 ± 211	395 ± 197.7	24.5 ± 68.5	168.2 ± 80.4

TABLE IX. The resonance poles on sheets II, IV, VIII, and XVI for 11 states. $\sqrt{s_r} = E_r - i\Gamma_r/2$ in MeV is given.

	II		IV		VIII		XVI	
State	E_r	$\Gamma_r/2$	E_r	$\Gamma_r/2$	E_r	$\Gamma_r/2$	E_r	$\Gamma_r/2$
$f_2(1270)$	1282.1 ± 2.6	67.5 ± 4.2	1256.9 ± 3.5	99.6 ± 3.1	1276.8 ± 2.9	73.4 ± 3.9	1264.2 ± 3.4	98.0 ± 3.5
$f_2(1430)$	1425.1 ± 48.0	98.8 ± 54.0	1421.3 ± 49.2	109.3 ± 52.7	1425.5 ± 47.5	98.2 ± 55.2	1421.7 ± 49.3	108.8 ± 52.3
$f_2'(1525)$	1533.6 ± 13.4	24.2 ± 28.0	1533.7 ± 12.6	23.0 ± 29.0	1534.2 ± 12.6	17.3 ± 29.0	1534.1 ± 13.2	19.5 ± 28.0
$f_2(1565)$	1590.3 ± 44.3	80.5 ± 34.3	1591.6 ± 41.3	74.1 ± 34.4	1600.4 ± 41.0	23.0 ± 34.7	1601.1 ± 39.8	9.4 ± 35.0
$f_2(1730)$	1710.0 ± 11.5	87.0 ± 26.9	1710.6 ± 11.2	83.8 ± 26.8	1717.3 ± 9.6	42.4 ± 27.2	1718.1 ± 9.3	31.9 ± 27.3
$f_2(1810)$	1752.4 ± 25.7	78.9 ± 14.7	1751.8 ± 25.6	83.8 ± 14.7	1756.9 ± 25.2	50.6 ± 14.9	1758.0 ± 25.0	36.5 ± 14.8
$f_2(1960)$	1958.0 ± 42.9	50.0 ± 18.6	1957.2 ± 42.9	56.8 ± 18.5	1962.3 ± 42.2	3.5 ± 19.0	1961.9 ± 42.3	7.4 ± 19.1
$f_2(2000)$	2002.6 ± 35.9	84.3 ± 61.6	2004.0 ± 34.9	68.2 ± 64.1	2003.1 ± 35.3	82.1 ± 63.8	2001.8 ± 36.2	94.6 ± 61.6
$f_2(2020)$	2025.3 ± 39.0	52.2 ± 51.1	2025.6 ± 38.1	45.4 ± 56.9	2025.8 ± 37.9	42.5 ± 57.1	2025.3 ± 38.8	51.8 ± 51.3
$f_2(2240)$	2196.4 ± 62.3	102.8 ± 54.5	2196.9 ± 62.1	97.9 ± 55.4	2201.7 ± 61.3	24.0 ± 56.7	2201.1 ± 61.4	45.0 ± 56.5
$f_2(2410)$	2385.1 ± 48.5	71.3 ± 58.3	2387.0 ± 47.3	5.6 ± 60.6	2387.0 ± 47.8	18.7 ± 60.4	2384.5 ± 48.7	83.8 ± 58.5

which correspond the following signs of analytic continuations of the quantities $\mathrm{Im}\sqrt{s-s_1}$, $\mathrm{Im}\sqrt{s-s_2}$, $\mathrm{Im}\sqrt{s-s_3}$, and $\mathrm{Im}\sqrt{s-s_4}$: $-+++$, $+-++$, $++-+$, and $+++-$, respectively, if one prolongs the numeration of sheets taken in Sec. II. In Table IX, the obtained poles on these sheets in the complex-energy plane $\sqrt{s}$ are shown for the case of 11 resonances. Errors of the pole positions are estimated using a Monte Carlo method. In the method, the parameters M_r and f_{rj} are randomly generated using a normal distribution (Gaussian) with the width given by the parameter error in Table VIII. Having generated the parameters, distributions (histograms for deviations of the pole positions) for the real and imaginary parts of the pole positions are evaluated and the standard deviations, which characterize ''widths'' of the distributions for the pole position, are calculated.

Finally, in Table X specified values of the masses m_{res} and total widths Γ_{tot} of states are given calculated from the pole positions using the resonance part of amplitude in the form (13). It is clear that the values of these quantities, calculated from the pole positions on various sheets, slightly differ from each other; for the $f_2(2240)$ and $f_2(2410)$, lying in the energy region where data are very scanty, even considerably. In Table X, there are shown only the values which match best the corresponding values M_r and an estimation of Γ_{tot} in Table VIII. The sheets on which the poles, used in calculation of these quantities, lie are also indicated. In those cases when two sheets are indicated, the pole positions on these sheets do not differ more than 1–1.5 MeV; however, the pole position on the first indicated sheet is shown.

VI. DISCUSSION AND CONCLUSIONS

First, let us emphasize an importance of the notion of the pole clusters (poles and zeros on the Riemann surface) as characteristics of multichannel states in the model-independent approach. This means that a multichannel resonance (depending on its nature) is represented by one of the types of pole clusters: 3 types in the 2-channel consideration and 7 types in the 3-channel one.

It is also shown in the example of the analysis of the isovector P wave of $\pi\pi$ scattering that it is impossible to obtain a reliable information on the multichannel resonances analyzing only the one process (see Tables I and III) though, looking over all possibilities of the resonance representations by the relevant pole clusters, one can extract a part of reliable information. But, in general, a combined analysis of data on the number of coupled processes is needed.

In the combined model-independent analysis of data on the $\pi\pi \to \pi\pi$, $K\bar{K}$, $\eta\eta$, and $\eta\eta'$ processes in the channel with $I^G J^{PC} = 0^+0^{++}$, an additional confirmation of the σ meson with mass 774 ± 15 MeV and width

TABLE X. The masses and total widths of the f_2 resonances (all in MeV).

	$f_2(1270)$	$f_2(1430)$	$f_2'(1525)$	$f_2(1565)$	$f_2(1730)$	$f_2(1810)$
m_{res}	1268.0 ± 3.4	1425.5 ± 49.2	1533.8 ± 13.4	1592.3 ± 44.3	1712.2 ± 11.6	1753.8 ± 25.6
Γ_{tot}	196.0 ± 7.0	218.6 ± 105.4	48.4 ± 56.0	161.0 ± 68.6	174.0 ± 53.8	167.6 ± 29.4
Sheet	XVI	IV, XVI	II, IV	II	II	IV
	$f_2(1960)$	$f_2(2000)$	$f_2(2020)$	$f_2(2240)$	$f_2(2410)$	
m_{res}	1958.0 ± 42.9	2004.0 ± 36.3	2026.0 ± 39.0	2198.8 ± 62.3	2386.0 ± 48.7	
Γ_{tot}	113.6 ± 37.0	189.2 ± 123.2	104.4 ± 102.2	205.6 ± 109.0	167.6 ± 117.0	
Sheet	IV	XVI	II, XVI	II	XVI	

988 ± 36 MeV is obtained (the pole position on sheet II is $596 - i494$ MeV). These values of mass and width, calculated with help of Eq. (13) from the pole position on sheet II, correspond the most to the Breit-Wigner values of Ref. [4] (analysis of several processes with pseudoscalar mesons) and [5] (GAMS Collaboration, analysis of the reaction $pp \to pp\pi^0\pi^0$). Note that this mass value is in remarkable accord with the prediction ($m_\sigma \approx m_\rho$) on the basis of mended symmetry by Weinberg [11]. As to the obtained pole position on sheet II, the result of this analysis generally confirms the one of our previous 2-channel model-independent analysis [7] of data on processes $\pi\pi \to \pi\pi$ and $K\bar{K}$. Our value of the real part of the pole is near the ones of many works (see [1] and from the recent works, e.g., Ref. [79] [BES Collaboration, analysis of the decay $\psi(2S) \to \pi^+\pi^- J/\psi$]. Our imaginary part of the $f_0(600)$-pole position is about 2 times larger than the one obtained in most indicated works. Note, however, that in the coupled-channel analyses of data on processes $\bar{p}p \to 3\pi^0$, $\pi^0\eta\eta$, and $\pi^0\pi^0\eta$ [47,48] (Crystal Barrel Collaboration) and on processes $\pi\pi \to \pi\pi$, $K\bar{K}$ [3], the obtained pole position on sheet II might be considered to be consistent with our one, especially with the imaginary part. Finally, let us indicate the positions of the discussed pole obtained in a straightforward calculation, based on the Roy equation for the isoscalar S wave [80], $\sqrt{s_\sigma} = 441^{+16}_{-8} - i272^{+18}_{-25}$ MeV, and in the recent dispersive analysis of data on only the $\pi\pi$ scattering [81]: $\sqrt{s_\sigma} = 461^{+14.5}_{-15.5} - i255 \pm 16$ MeV.

Some indication for $f_0(980)$ ($m_{\text{res}} = 1009.6$ MeV, $\Gamma_{\text{tot}} = 68.6$ MeV) is obtained to be the bound $\eta\eta$ state. However, one can see, considering the $f_0(980)$ listing in the PDG issue [1], that the mass of this state is obtained to be above the $K\bar{K}$ threshold in analyses of the $\pi\pi$ scattering, of the multichannel $\pi\pi$ scattering ($\pi\pi \to \pi\pi$, $K\bar{K}$, $\eta\eta$, and $\eta\eta'$) and of processes $\bar{p}p(n) \to M_1M_2M_3$, whereas below the $K\bar{K}$ threshold in analyses of the decays of D^+, B^+, J/ψ, and Z bosons, of processes $e^+e^- \to M_1M_2\gamma$, $\phi M_1M_2\gamma$, $e^+e^- M_1M_2$, M_1M_2X, and $pp \to ppM_1M_2$. Since the mass value below the $K\bar{K}$ threshold is important for a dynamical interpretation of the $f_0(980)$ as the $K\bar{K}$ molecule [26–28], it seems that the nature of this state is more complicated than the simply bound $\eta\eta$ state or $K\bar{K}$ molecule. From the point of view of quark structure, these two possibilities are the 4-quark states. It seems, this is consistent somehow with arguments in favor of the 4-quark nature of $f_0(980)$ in [82].

In our analysis, the $f_0(1370)$ and $f_0(1710)$ have the dominant $s\bar{s}$ component. Conclusion about the $f_0(1370)$ agrees quite well with the one drawn by the Crystal Barrel Collaboration [48], where the $f_0(1370)$ is identified as $\eta\eta$ resonance in the $\pi^0\eta\eta$ final state of the $\bar{p}p$ annihilation at rest. Conclusion about the $f_0(1710)$ is quite consistent with the experimental facts that this state is observed in $\gamma\gamma \to K_S\bar{K}_S$ [83] and not observed in $\gamma\gamma \to \pi^+\pi^-$ [84].

As to the $f_0(1500)$ ($m_{\text{res}} = 1511.4$ MeV, $\Gamma_{\text{tot}} = 397.6$ MeV), we suppose that it is practically the eighth component of the octet mixed with the glueball being dominant in this state. Its biggest width among the enclosing states tells also in favor of its glueball nature [54]. Note that in the PDG issue on the $f_0(1500)$ listing, the averaged value of width 109 ± 7 MeV is cited. However, there one indicates only the results of the analyses of mesons production and decay processes. In those few cases when the results of combined analyses of coupled processes are cited, authors did not use the representations of the multichannel resonances by pole clusters (this is especially important in the case of wide resonances), i.e., they did not apply all aspects of the multichannel analysis. On the other hand, one can see from data on the scattering processes, both analyzed here [67] and the alternative (one of the solutions of the phase analysis [75,76]), that energy dependences of observed quantities do not demonstrate a pronounced structure in the 1500-MeV region, which is needed for the narrow resonance. Therefore, it is reasonable to suggest that in this region there is a superposition of two states, wide and narrow. The latter is observed just in the processes of decay and the production of mesons.

We propose the following assignment of scalar mesons lying below 1.9 GeV to lower nonets, excluding the $f_0(980)$ as the $\eta\eta$ bound state. The lowest nonet: the isovector $a_0(980)$, the isodoublet $K_0^*(900)$, and $f_0(600)$ and $f_0(1370)$ as mixtures of the eighth component of octet and the SU(3) singlet. Then the GMO formula

$$3m_{f_8}^2 = 4m_{K_0^*}^2 - m_{a_0}^2, \tag{24}$$

gives $m_{f_8} = 872$ MeV ($m_\sigma = 774 \pm 14$ MeV). In the relation for masses of nonet

$$m_\sigma + m_{f_0(1370)} = 2m_{K_0^*}, \tag{25}$$

the left-hand side is about 21% bigger than the right-hand one.

The next nonet: $a_0(1450)$, $K_0^*(1450)$, and $f_0(1500)$ and $f_0(1710)$. From the GMO formula, we get $m_{f_8} \approx 1450$ MeV. In the relation

$$m_{f_0(1500)} + m_{f_0(1710)} = 2m_{K_0^*(1450)}, \tag{26}$$

the left-hand side is about 12% bigger than the right-hand one.

This assignment removes a number of questions, arisen earlier, and does not add new ones. Above all, this is related to the main one of them which consists of an impossibility to explain combined the approximately equal masses of the $f_0(980)$ and $a_0(980)$ and found $s\bar{s}$ dominance in the wave function of the $f_0(980)$. If these states are in the same nonet, the $f_0(980)$ must be heavier than $a_0(980)$ for 240–300 MeV, because the difference of masses of s and u quarks is 120–150 MeV. We proposed our way to solve this problem.

The mass formulas indicate a nonsimple mixing scheme. The breaking of relations (25) and (26) says that the $\sigma - f_0(1370)$ and $f_0(1500) - f_0(1710)$ systems get additional contributions absent in the $K_0^*(900)$ and $K_0^*(1450)$, respectively. A search of the adequate mixing scheme is complicated by the circumstance that there is also a remainder of the chiral symmetry, though, on the other hand, this permits one to predict correctly, e.g., the σ-meson mass [11].

In the vector sector, we used also the model-independent method. However, unlike our previous works [32,57] where we analyzed the 2-channel $\pi\pi$ scattering, in the present work we considered the 3-channel $\pi\pi$ scattering, i.e., we take into account the threshold of the third effective channel in the corresponding uniformizing variable. This threshold is found to be at about 1512.35 MeV and interpreted by us as related to the $\rho\sigma$ channel. Since the σ meson provokes many questions up to now it is interesting to observe the $\rho\sigma$ final state in the π-π collisions.

The values of mass (769.8 ± 0.3 MeV) and total width (144.9 ± 0.6 MeV) for the $\rho(770)$, obtained in this analysis, are a little bit smaller than the corresponding averaged values cited in the PDG tables [1], 775.49 ± 0.34 MeV and 149.4 ± 1.0 MeV, respectively. However, they also occur in the analysis of some reactions (see the PDG tables).

The first ρ-like meson has the mass 1274.7 ± 32.4 MeV and total width 304.3 ± 23.6 MeV. The indicated values of mass differ significantly from the mass (1459 ± 11 MeV) of the $\rho(1450)$ cited in the PDG issue as the first ρ-like meson, the value of mass of this state (obtained in various works) being indicated in the interval from 1250 to about 1580 MeV. As we discussed in the Introduction, the $\rho(1250)$, interpreted as the first radial excitation of the $\rho(770)$ state, and the isodoublet $K^*(1410)$ are well located to the octet of the first radial excitations. The mass of the latter should be by about 120–150 MeV larger than the mass of the former. Then the GMO formula gives for the mass of the eighth component of this octet the value of about 1460 MeV, that is fairly compatible with the mass of the first ω-like meson $\omega(1420)$, for which one obtains the values in the range 1350–1460 MeV in various works (see the PDG tables [1]).

Considering Tables I and III, one can see that the description with four resonances is a little better than that with five resonances though an existence of the $\rho(1450)$ [together with $\rho(1250)$] does not contradict the data. Therefore, taking into account that if the $\rho(1450)$ is considered as the $^3D_1$ $q\bar{q}$ state [32,57], the possible SU(3) partners [the isodoublet $K^*(1680)$ and the isoscalars $\omega(1650)$ and $\phi(1680)$] can be found, and we prefer the five-resonance scenario for the description of data [65–67] on the isovector P wave of $\pi\pi$ scattering below 1880 MeV. In our analysis this state has $m_{\rm res} = 1429.8 \pm 26.3$ MeV and $\Gamma_{\rm tot} = 232.5 \pm 48.6$ MeV.

The third ρ-like meson ($m_{\rm res} = 1595.3 \pm 5.4$ MeV and $\Gamma_{\rm tot} = 128.5 \pm 7.7$ MeV) corresponds well to the recent observation [85] (*BABAR* Collaboration) of the $\rho(1570)$ with mass 1570 ± 36 ± 62 MeV and width 144 ± 75 ± 43 MeV in the process $e^+e^- \to \phi\pi^0\gamma$ (see also the PDG tables [1]). It seems that it is possible to find the SU(3) partners for this state in accessible analyses of various data, e.g., in the PDG issue on the $K^*(1680)$ listing, the LASS Collaboration results of the observation of different reactions $K^- p \to K^-\pi^+ n$ and $K^- p \to \bar{K}^0\pi^+\pi^- n$. In the first case, the state was observed with the mass 1677 ± 10 ± 32 MeV and width 205 ± 16 ± 34 MeV and in the second case, with the mass 1735 ± 10 ± 20 MeV and width 423 ± 18 ± 30 MeV. We see that resonance parameters differ very noticeably. Are these parameters related to the different resonances? When taking this, the mass value 1735 MeV is acceptable to put this isodoublet $K^*(1735)$ into the octet with the $\rho(1600)$. Then from the GMO formula, we would expect for the mass of the eighth component of this octet the value 1779 MeV that quite corresponds to the results of some works cited in the PDG issue on the $\omega(1650)$ listing, where the mass values are indicated from 1606 to 1840 MeV; the analysis [86] of data [87] on $e^+e^- \to K_S^0 K^\pm\pi^\mp$ gives even the mass value about 2100 MeV.

The fourth ρ-like state, observed in the $\pi\pi$ scattering, has $m_{\rm res} = 1787 \pm 32.5$ MeV and $\Gamma_{\rm tot} = 197.4 \pm 13.7$ MeV. These are consistent with the results of some works cited in the PDG issue on the $\rho(1700)$ listing, e.g., with the parameters of the ρ-like state, observed in the $e^+e^- \to \pi\pi$ process [88]. Note that in the present analysis of the 3-channel $\pi\pi$ scattering, the mass value of the fourth ρ-like state is diminished by about 100 MeV in comparison with the analysis of the 2-channel $\pi\pi$ scattering [32,57].

In the tensor sector, we carried out two analyses—without and with the $f_2(2020)$. We do not obtain $f_2(1640)$, $f_2(1910)$, and $f_2(2150)$; however, we see $f_2(1450)$ and $f_2(1730)$ which are related to the statistically valued experimental points.

Usually one assigns the states $f_2(1270)$ and $f_2'(1525)$ to the ground tensor nonet. To the second nonet, one could assign the $f_2(1600)$ and $f_2(1760)$ though for now the isodoublet member is not discovered. If the $a_2(1730)$ is the isovector of this octet and if the $f_2(1600)$ is almost its eighth component, then, from the GMO formula, we expect this isodoublet mass at about 1633 MeV. Then the relation for masses of the nonet would be fulfilled with a 3% accuracy. Karnaukhov *et al.* [89] observed the strange isodoublet with yet indefinite remaining quantum numbers and with mass 1629 ± 7 MeV in the mode $K_s^0\pi^+\pi^-$. This state might be the tensor isodoublet of the second nonet.

The states $f_2(1963)$ and $f_2(2207)$ together with the isodoublet $K_2^*(1980)$ could be put into the third nonet. Then in the relation for masses of nonet

$$m_{f_2(1963)} + m_{f_2(2207)} = 2m_{K_2^*(1980)}, \tag{27}$$

the left-hand side is only 5.3% bigger than the right-hand

one. If one considers $f_2(1963)$ as the eighth component of the octet, the GMO formula

$$m^2_{a_2} = 4m^2_{K^*_2(1980)} - 3m^2_{f_2(1963)} \tag{28}$$

gives $m_{a_2} = 2030$ MeV. This value coincides with the one for the a_2 meson obtained in [90]. This state is interpreted as the second radial excitation of the 1^-2^{++} state on the basis of consideration of the a_2 trajectory on the (n, m^2) plane (n is the radial quantum number of the $q\bar{q}$ state) [64].

As to the $f_2(2000)$, the presence of the $f_2(2020)$ in the analysis with 11 resonances helps to interpret the $f_2(2000)$ as a glueball. In the case of ten resonances, the ratio of the $\pi\pi$ and $\eta\eta$ widths is in the limits obtained in Ref. [64] for the tensor glueball on the basis of the $1/N_c$-expansion rules. However, the $K\bar{K}$ width is too large for the glueball. At practically the same description of processes with the consideration of 11 resonances as in the case of ten, their parameters have varied a little, except for the $f_2(2000)$ and $f_2(2410)$. The mass of the latter has decreased by about 40 MeV. As to the $f_2(2000)$, its $K\bar{K}$ width has changed significantly. Now all the obtained ratios of the partial widths are in the limits corresponding to the glueball.

The question of interpretation of the $f_2(1450)$, $f_2(1730)$, $f_2(2020)$, and $f_2(2410)$ is generally open. It could be supposed that at least the first three states are of a non-$q\bar{q}$ nature. However, the first two states cannot be either glueballs or $q\bar{q}g$ hybrids. One can, therefore, think that these states are the 4-quark ones. Then for the isodoublet mass of the corresponding nonet, we would expect the value about 1570–1600 MeV. Unfortunately, for now we do not know experimental indications for the tensor isodoublet of that mass. However, note that in the known experimental spectrum of the K^*_2 family, there is a 500-MeV unoccupied gap from 1470 to 1970 MeV [1], except for the above work [89]. Note also that, as one can see in the PDG tables on the $a_2(1700)$ listing, the observed isovector tensor states in the 1660–1775-MeV interval differ in the width by about 2–3 times, i.e., possess various properties. For example, the broad state, observed in the process $\bar{p}p \to \eta\eta\pi^0$ [91] (FNAL E835) with mass 1702 ± 7 MeV and width 417 ± 19 MeV, might be the isovector member of the corresponding 4-quark nonet. Of course, the assumption of this 4-quark possibility presupposes an existence of the scalar 4-quark states at lower energies which are not seen in the analysis. One can think that these states are a part of the background due to their very large widths.

ACKNOWLEDGMENTS

The authors are grateful to S. B. Gerasimov, T. Gutsche, M. A. Ivanov, and V. E. Lyubovitskij for useful discussions and interest in this work. The work has been supported by the Votruba-Blokhintsev Program for Cooperation of the Czech Republic with JINR (Dubna), the Grant Agency of the Czech Republic (Grant No. 202/08/0984), the Slovak Scientific Grant Agency (Grant VEGA No. 2/0034/09), and the Bogoliubov-Infeld Program for Cooperation of Poland with JINR (Dubna).

[1] C. Amsler *et al.* (PDG Collaboration), Phys. Lett. B **667**, 1 (2008).
[2] Yu. Troyan *et al.*, JINR Rapid Communications **5–91**, 33 (1998).
[3] P. Estabrooks, Phys. Rev. D **19**, 2678 (1979).
[4] N. A. Törnqvist and M. Roos, Phys. Rev. Lett. **76**, 1575 (1996).
[5] D. M. Alde *et al.*, Phys. Lett. B **397**, 350 (1997).
[6] Yu. S. Surovtsev, D. Krupa, and M. Nagy, Phys. Rev. D **63**, 054024 (2001).
[7] Yu. S. Surovtsev, D. Krupa, and M. Nagy, Eur. Phys. J. A **15**, 409 (2002).
[8] Yu. S. Surovtsev, D. Krupa, and M. Nagy, AIP Conf. Proc. **717**, 357 (2004).
[9] Yu. S. Surovtsev, D. Krupa, and M. Nagy, Czech. J. Phys. **56**, 807 (2006).
[10] Yu. S. Surovtsev and R. Kamiński, Frascati Phys. Series **46**, 669 2007).
[11] S. Weinberg, Phys. Rev. Lett. **65**, 1177 (1990).
[12] F. J. Gilman and H. Harari, Phys. Rev. **165**, 1803 (1968).
[13] R. Kamiński, G. Mennessier, and S. Narison, Phys. Lett. B **680**, 148 (2009).
[14] C. McNeile, Nucl. Phys. B, Proc. Suppl. **186**, 264 (2009).
[15] Y. Chen *et al.*, Phys. Rev. D **73**, 014516 (2006).
[16] J. Ellis and J. Lánik, Phys. Lett. **150B**, 289 (1985).
[17] V. V. Anisovich, Phys. Usp. **41**, 419 (1998); V. V. Anisovich, D. V. Bugg, and A. V. Sarantsev, Phys. Rev. D **58**, 111503(R) (1998).
[18] F. Giacosa, T. Gutsche, V. E. Lyubovitskij, and A. Faessler, Phys. Rev. D **72**, 094006 (2005).
[19] C. Amsler and F. E. Close, Phys. Rev. D **53**, 295 (1996).
[20] D. Morgan, Phys. Lett. **51B**, 71 (1974).
[21] N. A. Törnqvist, Phys. Rev. Lett. **49**, 624 (1982).
[22] J. Lánik, Phys. Lett. B **306**, 139 (1993).
[23] N. A. Törnqvist and M. Roos, Phys. Rev. Lett. **76**, 1575 (1996).
[24] R. L. Jaffe, Phys. Rev. D **15**, 267 (1977); **15**, 281 (1977).
[25] N. N. Achasov, S. A. Devyanin, and G. N. Shestakov, Phys. Lett. **96B**, 168 (1980); Z. Phys. C **22**, 53 (1984).
[26] J. Weinstein and N. Isgur, Phys. Rev. Lett. **48**, 659 (1982); Phys. Rev. D **27**, 588 (1983); **41**, 2236 (1990).
[27] G. Janssen, B. C. Pearce, K. Holinde, and J. Speth, Phys. Rev. D **52**, 2690 (1995).
[28] T. Branz, T. Gutsche, and V. E. Lyubovitskij, Eur. Phys. J. A **37**, 303 (2008).

[29] R. L. Jaffe and K. Johnson, Phys. Lett. **60B**, 201 (1976); T. Barnes, F. E. Close, and S. Monoghan, Nucl. Phys. **B198**, 380 (1982).
[30] N. N. Achasov, Nucl. Phys. **A675**, 279 (2000).
[31] M. N. Achasov *et al.*, Phys. Lett. B **438**, 441 (1998); **440**, 442 (1998).
[32] Yu. S. Surovtsev, P. Bydžovský, R. Kamiński, and M. Nagy, Int. J. Mod. Phys. A **24**, 586 (2009).
[33] P. Minkowski and W. Ochs, Eur. Phys. J. C **9**, 283 (1999); Nucl. Phys. B, Proc. Suppl. **121**, 119 (2003); **121**, 123 (2003).
[34] D. Bugg, Eur. Phys. J. C **52**, 55 (2007); arXiv:0710.4452.
[35] C. Amsler *et al.*, Phys. Lett. B **291**, 347 (1992).
[36] A. Abele *et al.*, Nucl. Phys. **A609**, 562 (1996).
[37] M. Ablikim *et al.*, Phys. Lett. B **607**, 243 (2005).
[38] D. Alde *et al.*, Eur. Phys. J. A **3**, 361 (1998).
[39] R. Molina, D. Nicmorus, and E. Oset, Phys. Rev. D **78**, 114018 (2008).
[40] D. Krupa, V. A. Meshcheryakov, and Yu. S. Surovtsev, Nuovo Cimento Soc. Ital. Fis. A **109**, 281 (1996).
[41] V. V. Anisovich *et al.*, Phys. At. Nucl. **63**, 1410 (2000); V. V. Anisovich, V. A. Nikonov, and A. V. Sarantsev, Phys. At. Nucl. **65**, 1545 (2002).
[42] D. Alde *et al.*, Z. Phys. C **66**, 375 (1995); Yu. D. Prokoshkin, A. A. Kondashov, and S. A. Sadovsky, Dokl. Akad. Nauk Ser. Fiz. **342**, 473 (1995).
[43] F. G. Binon *et al.*, Nuovo Cimento Soc. Ital. Fis. A **78**, 313 (1983).
[44] F. Binon *et al.*, Nuovo Cimento Soc. Ital. Fis. A **80**, 363 (1984).
[45] S. J. Lindenbaum and R. S. Longacre, Phys. Lett. B **274**, 492 (1992); A. Etkin *et al.*, Phys. Rev. D **25**, 1786 (1982).
[46] V. V. Anisovich *et al.*, Phys. Lett. B **323**, 233 (1994).
[47] C. Amsler *et al.*, Phys. Lett. B **342**, 433 (1995).
[48] C. Amsler *et al.*, Phys. Lett. B **355**, 425 (1995).
[49] F. E. Close and A. Kirk, Eur. Phys. J. C **21**, 531 (2001).
[50] S. Narison, Nucl. Phys. **B509**, 312 (1998).
[51] A. V. Anisovich, V. V. Anisovich, and A. V. Sarantsev, Phys. Rev. D **62**, 051502(R) (2000).
[52] S. Godfrey and N. Isgur, Phys. Rev. D **32**, 189 (1985).
[53] N. A. Törnqvist, arXiv:hep-ph/0204215.
[54] A. V. Anisovich, V. V. Anisovich, Yu. D. Prokoshkin, and A. V. Sarantsev, Nucl. Phys. B, Proc. Suppl. **56**, 270 (1997).
[55] F. E. Close and N. A. Törnqvist, J. Phys. G **28**, R249 (2002).
[56] M. K. Volkov and V. L. Yudichev, Yad. Fiz. **65**, 1701 (2002).
[57] Yu. S. Surovtsev and P. Bydžovský, Frascati Phys. Series **46**, 1535 (2007); Nucl. Phys. **A807**, 145 (2008).
[58] I. Yamauchi and T. Komada, Frascati Phys. Series **46**, 445 (2007).
[59] N. M. Budnev *et al.*, Phys. Lett. **70B**, 365 (1977).
[60] S. B. Gerasimov and A. B. Govorkov, Z. Phys. C **13**, 43 (1982); **29**, 61 (1985).
[61] D. Aston *et al.*, Nucl. Phys. B, Proc. Suppl. **21**, 105 (1991).
[62] V. K. Henner and T. S. Belozerova, Phys. Part. Nucl. **29**, 63 (1998).
[63] E. van Beveren, G. Rupp, T. A. Rijken, and C. Dullemond, Phys. Rev. D **27**, 1527 (1983).
[64] V. V. Anisovich *et al.*, Int. J. Mod. Phys. A **20**, 6327 (2005).
[65] S. D. Protopopescu *et al.*, Phys. Rev. D **7**, 1279 (1973).
[66] P. Estabrooks and A. D. Martin, Nucl. Phys. **B79**, 301 (1974).
[67] B. Hyams *et al.*, Nucl. Phys. **B64**, 134 (1973); **B100**, 205 (1975).
[68] A. Zylbersztejn *et al.*, Phys. Lett. **38B**, 457 (1972); P. Sonderegger and P. Bonamy, in Proceedings of the 5th International Conference on Elementary Particles, Lund, 1969, paper 372; J. R. Bensinger *et al.*, Phys. Lett. **36B**, 134 (1971); J. P. Baton *et al.*, Phys. Lett. **33B**, 525 (1970); **33B**, 528 (1970); P. Baillon *et al.*, Phys. Lett. **38B**, 555 (1972); L. Rosselet *et al.*, Phys. Rev. D **15**, 574 (1977); A. A. Kartamyshev *et al.*, Pis'ma Zh. Eksp. Teor. Fiz. **25**, 68 (1977); A. A. Bel'kov *et al.*, Pis'ma Zh. Eksp. Teor. Fiz. **29**, 652 (1979).
[69] W. Wetzel *et al.*, Nucl. Phys. **B115**, 208 (1976); V. A. Polychronakos *et al.*, Phys. Rev. D **19**, 1317 (1979); P. Estabrooks, Phys. Rev. D **19**, 2678 (1979); D. Cohen *et al.*, Phys. Rev. D **22**, 2595 (1980); G. Costa *et al.*, Nucl. Phys. **B175**, 402 (1980); A. Etkin *et al.*, Phys. Rev. D **25**, 1786 (1982).
[70] S. J. Lindenbaum and R. S. Longacre, Phys. Lett. B **274**, 492 (1992); R. S. Longacre *et al.*, Phys. Lett. B **177**, 223 (1986).
[71] K. J. Le Couteur, Proc. R. Soc. A **256**, 115 (1960); R. G. Newton, J. Math. Phys. (N.Y.) **2**, 188 (1961); M. Kato, Ann. Phys. (N.Y.) **31**, 130 (1965).
[72] J. Bohacik and H. Kühnelt, Phys. Rev. D **21**, 1342 (1980).
[73] D. Morgan and M. R. Pennington, Phys. Rev. D **48**, 1185 (1993).
[74] N. N. Achasov and G. N. Shestakov, Phys. Rev. D **49**, 5779 (1994).
[75] G. Grayer *et al.*, Nucl. Phys. **B75**, 189 (1974).
[76] R. Kaminski, L. Lesniak, and K. Rybicki, Z. Phys. C **74**, 79 (1997).
[77] S. Ishida *et al.*, Prog. Theor. Phys. **95**, 745 (1996); **98**, 621 (1997).
[78] B. S. Zou and D. V. Bugg, Phys. Rev. D **48**, R3948 (1993).
[79] M. Ablikim *et al.*, Phys. Lett. B **645**, 19 (2007).
[80] I. Caprini, G. Colangelo, and H. Leutwyler, Phys. Rev. Lett. **96**, 132001 (2006).
[81] R. Kaminski, R. Garcia-Martin, P. Grynkiewicz, and J. R. Pelaez, Nucl. Phys. B, Proc. Suppl. **186**, 318 (2009).
[82] N. N. Achasov, Nucl. Phys. **A675**, 279 (2000); M. N. Achasov *et al.*, Phys. Lett. B **438**, 441 (1998); **440**, 442 (1998).
[83] S. Braccini, Frascati Phys. Series **15**, 53 (1999).
[84] R. Barate *et al.*, Phys. Lett. B **472**, 189 (2000).
[85] B. Aubert *et al.*, Phys. Rev. D **77**, 092002 (2008).
[86] N. N. Achasov and A. A. Kozhevnikov, Phys. Rev. D **57**, 4334 (1998).
[87] D. Bisello *et al.*, Z. Phys. C **52**, 227 (1991).
[88] D. Bisello *et al.*, Phys. Lett. B **220**, 321 (1989).
[89] V. M. Karnaukhov, V. I. Moroz, and C. Coca, Yad. Fiz. **63**, 652 (2000).
[90] A. V. Anisovich *et al.*, Phys. Lett. B **452**, 173 (1999); **452**, 187 (1999); **517**, 261 (2001).
[91] I. Uman *et al.*, Phys. Rev. D **73**, 052009 (2006).